Carbon and Graphene Quantum Dots for Optoelectronic and Energy Devices: A Review

*Xiaoming Li, Muchen Rui, Jizhong Song, Zihan Shen, and Haibo Zeng**

As new members of carbon material family, carbon and graphene quantum dots (CDs, GQDs) have attracted tremendous attentions for their potentials for biological, optoelectronic, and energy related applications. Among these applications, bio-imaging has been intensively studied, but optoelectronic and energy devices are rapidly rising. In this Feature Article, recent exciting progresses on CD- and GQD-based optoelectronic and energy devices, such as light emitting diodes (LEDs), solar cells (SCs), photodetctors (PDs), photocatalysis, batteries, and supercapacitors are highlighted. The recent understanding on their microstructure and optical properties are briefly introduced in the first part. Some important progresses on optoelectronic and energy devices are then addressed as the main part of this Feature Article. Finally, a brief outlook is given, pointing out that CDs and GQDs could play more important roles in communication- and energy-functional devices in the near future.

1. Introduction

As one of the essential elements of the organism, industry and society, carbon always occupies an important position in the development of modern science and technology. From graphite to carbon nanotube and fullerene, the carbon family ushered in two new members, graphene,[1] and luminescent carbon materials,[2] in 2004. Because of the excellent electrical, mechanical, and optical properties, graphene has aroused numerous attentions in the past decade and even won the Nobel Prize in 2010.[3–7] However, luminescent carbon materials, carbon dots (CDs), were not synthesized in large quantities until 2006.[8] This work caused a boom in research through the whole world because of their merits, such as high luminesce and upconversion luminescence,[9] chemical stability, dispersibility in water, low photobleaching, biocompatibility, low cost, and low toxicity. These interesting properties make them new-generation luminescent materials superior to conventionally used fluorescent organic dyes and luminescent inorganic quantum dots. In 2010, Pan et al. successfully cut graphene sheets into blue luminescent graphene quantum dots via hydrothermal route, pushing the research of luminescent carbon materials to a climax.[10] Before that, much work has been done in the field of bioimaging and optical sensing[11–13] while little research can be found in the optoelectronic devices or energy related applications. Since 2010, attempts on multiple applications, such as photovoltaic devices,[14–18] light emitting diodes,[19–22] photodetectors,[23,24] photocatalysis,[25] and lithium ion batteries,[26,27] were made. CDs and GQDs are gradually emerging in these areas and improving the performance of some kinds of devices with facile methods and low cost.

Actually, GQDs can be recognized as one kind of CDs, which usually possess better crystallinity than its cousins.[28,29] In spite of the controversies on the origin of luminescence due to the excitation-dependent behavior, CDs and GQDs are expected to lead to low cost solar cells and organic LEDs (OLEDs)[16] and even can improve the performance of supercapacitors[27] and lithium ion batteries (LIBs) greatly.[26] Both of them have been synthesized with various methods, including top-down and bottom-up approaches. We are not going to talk about this because some reviews have concluded them.[30–32] In this Feature Article, we would like to update the latest researches about the applications of CDs and GQDs in optoelectronic devices and energy related devices, as shown in **Figure 1**. Besides, there are no specific reviews that focus on the applications of CDs and GQDs in optoelectronic devices up to date though they have been studied for several years. In the next section, we will make a brief introduction of the microstructure and optical properties of these luminescent carbon materials. Section 3 covers the multiple applications of these interesting materials. We will focus on the application for optoelectronic and energy-related devices and make a brief introduction of other applications. In Section 4, we give a perspective for CDs and GQDs, including potential applications and possible development trend. In view of several excellent reviews focusing on different aspects of CDs and GQDs, such as their synthesis, biological applications,[30] photoluminescent properties and environmental applications, we hope this article will provide valuable insights for the current statues of CDs and GQDs research in optoelectronics and energy and stimulate new ideas and further research on their potential applications.

X. M. Li, M. C. Rui, J. Z. Song, Z. H. Shen,
Prof. H. B. Zeng
Institute of Optoelectronics & Nanomaterials
College of Material Science and Engineering
Nanjing University of Science and Technology
Nanjing 210094, China
E-mail: zeng.haibo@njust.edu.cn

X. M. Li
State Key Laboratory of Mechanics and Control
of Mechanical Structures & College of Materials Science and Technology
Nanjing University of Aeronautics and Astronautics
Nanjing 210016, China

DOI: 10.1002/adfm.201501250

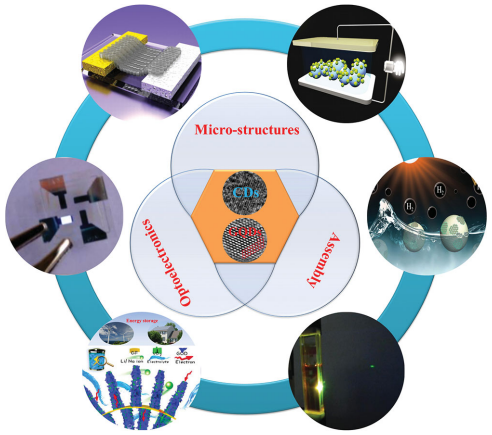

Figure 1. Illustration of the main topics of this Feature Article, showing the recent tendency of applications of CDs and GQDs in communication- and energy-functional devices, including LEDs, photodetectors, solar cells, lasing, photocatalysis, and energy related devices. Reprinted with permission.[17,21,24,26,90,116] Copyright 2012, 2014, Royal Society of Chemistry. Copyright 2014, 2015, American Chemical Society. Copyright 2014, Wiley-VCH.

2. Microstructure and Optical Properties

2.1. Microstructure of CDs and GQDs

Though GQDs can be considered as one kind of CDs, CDs usually possess distinct structure. Generally, CDs are quasi-spherical nanoparticles consisting of amorphous and crystalline parts.[29] Despite the fact that many researchers demonstrate the existence of crystalline sp^2 carbon section,[33,34] they possess poorer crystallinity than GQDs. In contrast, most of the GQDs are produced from graphene,[10] graphene oxide (GO),[35–37] and molecules with specific structure such as benzene rings.[28,36] Thus, GQDs usually have graphene lattices inside the dots, resembling the crystalline structure of single or few layered graphene. Interestingly, though CDs and GQDs own different core structures, both of them are functionalized with complex surface groups, especially oxygen related functional groups, such as carboxyl and hydroxyl.[38–42] These surface groups make great contributions to the optical properties of CDs and GQDs and also make them aqueous dispersible. Whilst, heteroatoms, such as nitrogen, sulfur and other elements enhance the luminescence and electrical conductivity of CDs and GQDs greatly[33,43–45] via tuning the electronic structures.

2.2. Optical Properties

From the accidental discovery of luminescent carbon materials, optical properties are the most frequently studied issues. Various CDs and GQDs with different PL color, ranging from UV to visible light and even near infrared region, have been synthesized with various approaches till now.[46–49] However, optical properties of CDs and GQDs are also the most controversial issues, such as the luminescence mechanism. The debate about luminescence origin comes from the interesting while confused excitation dependent behavior (**Figure 2**a–c), that is, the emission peak can vary according to the excitation wavelength.[8] Inconsistent experimental observations from the same synthesis as well as distinct but not precisely defined properties obtained from different approaches make the origin of luminescence more complicated. For instance, the proposed quantum confinement effect is not always observed[45] and precise control of experimental process is currently lack. Though more researches are needed to draw a clear picture of the luminescence mechanism, two classes of emission routes, intrinsic (band-gap related) and extrinsic (surface related) recombination routes, are widely accepted according to the literature.

First, similar pH dependent behavior is always observed that the luminescence intensity decreases at both high and low pH because of deprotonation and protonation, as seen in Figure 2d.[41,50] Sometimes, the emission wavelength even changes.[51] It means that the luminescence of CDs and GQDs are often related to the surface functional groups, such as carboxyl and hydroxyl groups.[41] Besides, reduction or oxidation of these groups may affect the optical properties totally, resulting in different visible light and PL intensity (Figure 2e).[19,39,52] Jin et al. demonstrated that both experimental and calculations from density functional theory proved the decrease of band gap

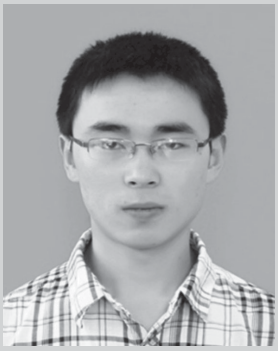

Xiaoming Li received his bachelor degree in Material Science from Nanjing University of Aeronautics and Astronautics in 2013. Now, he is a gruduate student in Prof. Zeng's group. His current research interests include luminescent materials and their applications.

Haibo Zeng obtained his Ph.D. in Material Physics from Institute of Solid State Physics in Chinese Academy of Sciences in 2006. Following visiting scholar at University of Karlsruhe (with Professor Claus Klingshirn and Professor Heinz Kalt) and then postdoctoral work at National Institute for Materials Science (with Professor Yoshio Bando and Professor Dmitri Golberg), he joined the faculty at Nanjing University of Science and Technology in 2011 and initiated the Institute of Optoelectronics & Nanomaterials in 2013. His research interests are focused on the exploratory design of semiconducting nanocrystals and two-dimensional crystals, with an emphasis on optoelectronic applications.

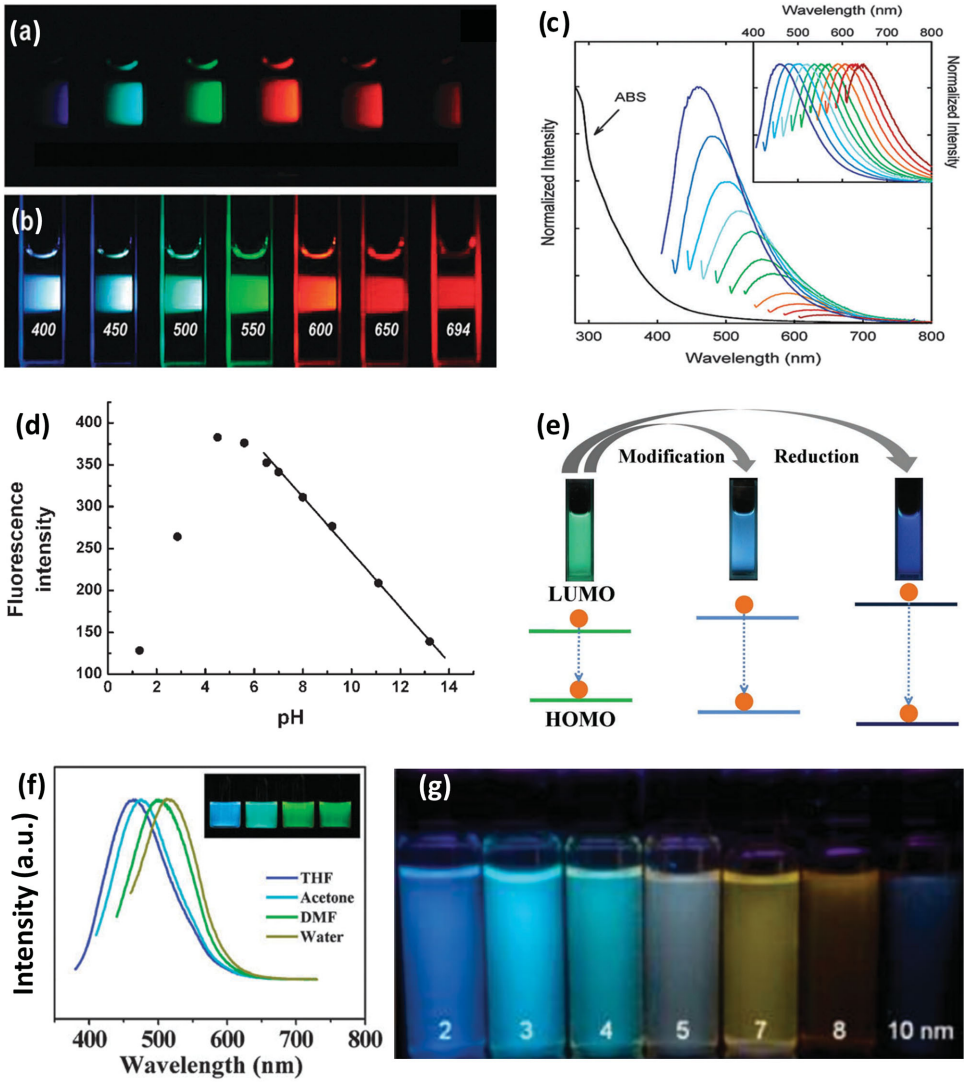

Figure 2. Recent progresses on the basic optical properties of CDs and GQDs. CDs a) excited at 400 nm and photographed through band-pass filters of different wavelengths as indicated, and b) excited at the indicated wavelengths and photographed directly. c) The absorption and excitation dependent photoluminescence spectra of CDs. Reprinted with permission.[8] Copyright 2006, American Chemical Society. d) Effect of the solution pH on the fluorescence intensity of CDs. Reprinted with permission.[56] Copyright 2008, Royal Society of Chemistry. e) Bandgap changing of GQDs after modification and reduction. Reprinted with permission.[39] Copyright 2012, Wiley-VCH. f) Effect of solvents on the fluorescence of GQDs. Reprinted with permission.[57] Copyright 2011, Royal Society of Chemistry. g) Photo of a series of the GQDs with various sizes under a 365 nm UV lamp. The captions represent the size of the GQDs. Reprinted with permission.[21] Copyright 2014, American Chemical Society.

via tuning the concentration of attached amino groups.[53] The change of band gap derives from the charge transfers between functional groups and GQDs. These works confirm the important roles of surface groups in the photoluminescence of CDs and GQDs. Bao et al. developed an electrochemical method to prepare CDs with narrow size distribution.[42] Surface oxidation of CDs can be controlled only by adjusting the applied potentials and red-shifted emission was observed for the CDs with a high surface oxidation degree. Those surface groups were claimed to introduce different emission sites onto CDs, which can trap excitons. Thereafter, the radiation from recombination of trapped excitons leads to the variation and red-shift of emission. This conclusion is consistent with the results of Shang et al. that oxidized carbon results in localized electronic states and the emission is predominantly from the electron transitions among/between the non-oxidized and oxidized carbon region.[54] However, how do these groups result in multicolor emissions is still in the air. What is certain is that emission lights cover the entire visible region can be achieved facilely via controlling the reaction processes and the final surface states.[55]

Lately, ultrafast time-resolved fluorescence and carrier dynamics of CDs were studied by Wen and co-workers.[58] The experiments reveal that the luminescence of CDs consists of two spectral overlapped bands. The intrinsic and extrinsic bands originate from sp^2 domains and surface states contribute the fluorescence of CDs. A fast trapping was observed from the sp^2-domains into the surface states with a time constant

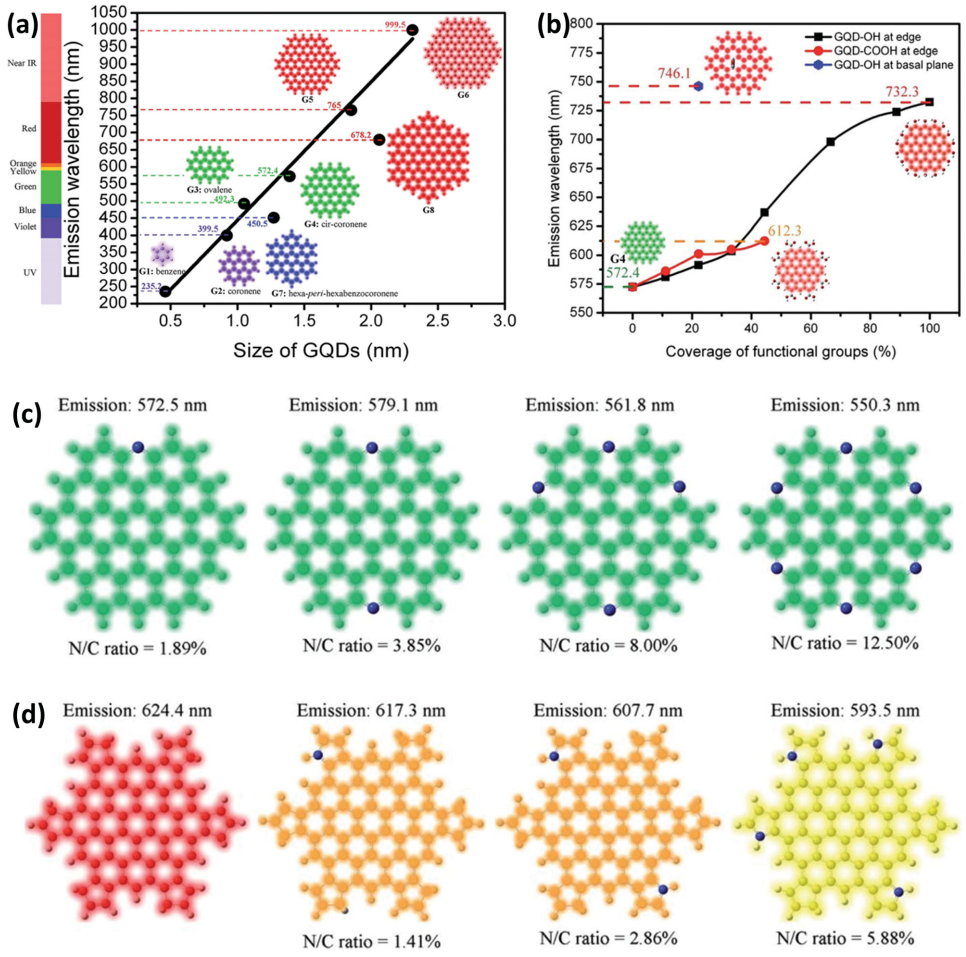

Figure 3. Recent progresses on the microstructure and electronic structure of CDs and GQDs. a) Calculated emission wavelength (nm) using TDDFT method in vacuum as a function of the diameter of GQDs. b) Emission wavelength of oxidized GQD (G4) as a function of the coverage of –OH and–COOH groups. c) N-doped GQDs with c) pyridine-like and d) pyrrolic nitrogen. Reprinted with permission.[62] Copyright 2014, Royal Society of Chemistry.

of 400 fs and the excitation dependent fluorescence can be ascribed to the abundant functional groups on the surface. Wang et al. also observed similar results with ultrafast spectroscopy that the common origin of blue and green light of CDs and GQDs are dominated with the competition among different emission centers and traps.[41,59] Regarding with the surface states including functional groups, interstitial atoms and vacancies, Liu et al. prepared GQDs with pure carbon structure and little functional groups. The fast recombination and optimized excitation in short wavelength makes the conclusion that blue emission originates from the intrinsic states with carbon crystalline structure more explicit.[60] In addition, the surface trapping from the nano domains is not the only resource for luminescence. The thermally distributed carriers can be directly trapped into the surface states, making contributions to the excitation dependent behavior.[58]

It is reported that the PL of GQDs and CDs is sensitive to solvent, as shown in Figure 2f, which is induced by solvent attachment or different emissive traps on the surface of GQDs.[57] In fact, in our opinion, solvents with different polarities will change the conjugation degree of sp^2 carbons, leading to different energy gaps, as well as various emissions. The changed optical properties indicate the contribution of transitions from conjugated π-domains. Therefore, the size of sp^2 domains within the sp^3 matrix is the real domination of quantum confinement effect and bright red emission can be obtained through cutting graphite into CDs with large sp^2 clusters.[49,61] The experimental results of quantum confinement effect have been observed by several groups. Kang group separated the CDs by column chromatography to obtain samples with different size and blue, green, yellow, and red PL was strong enough to be seen with the naked eyes.[34] Their theoretical calculations based on the size of sp^2 domains agreed well with the optical results. Kwon et al. obtained GQDs with controllable size in oil phase and the size dependent PL was obvious (Figure 2g).[21]

Recently, Sk et al. carried out theoretical analysis on the luminescence mechanism of GQDs using density-functional theory (DFT) and time-dependent DFT calculations. They find out that the PL of a GQD can be sensitively tuned by its size, edge configuration, shape, attached chemical functionalities, heteroatom doping and defects (**Figure 3**).[62] When GQDs were functionalized with bulky Fréchet's dendritic wedges at the GQD

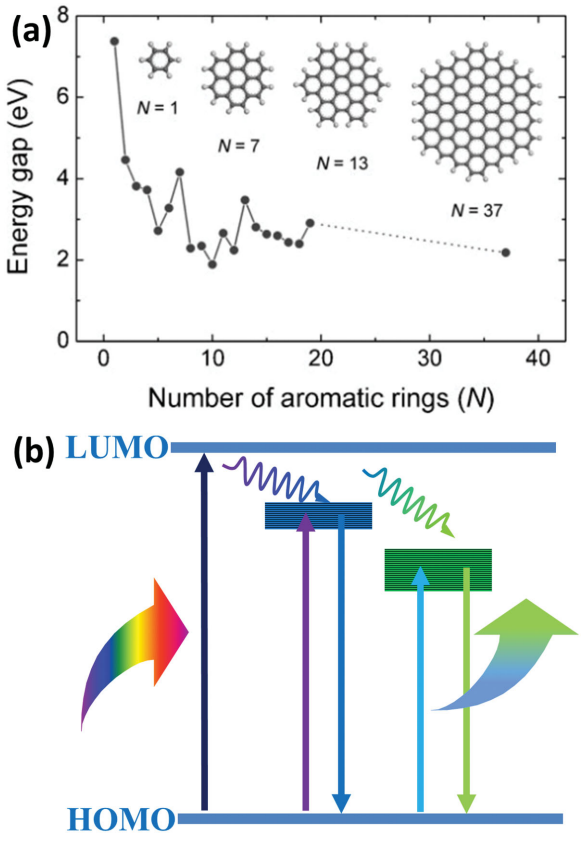

Figure 4. Recent progresses on the microstructure and electronic structure of CDs and GQDs. a) Energy gap of π–π^* transitions calculated based on DFT as a function of the number of aromatic rings. Reprinted with permission.[61] Copyright 2010, Wiley-VCH. b) Schematic of the proposed luminescence mechanism.

periphery, uncommon white light emission was obtained.[63] Similarly, highly fluorescent CDs with tunable visible emission from blue to red were synthesized by controlling doping and crystallinity (the size of sp^2 domains).[48] Therefore, though the in-depth luminescence origin of CDs and GQDs is still debatable, we can make preliminary conclusion that both the intrinsic and extrinsic states contribute to the luminescence. First of all, quantum confinement effect reflects in the size of sp^2 domains rather than particle size, as shown in **Figure 4**a. On one hand, after the excitation, excited carriers are trapped by surface states resulted from defects and oxidized carbons and emit light through irradiative recombination decay. On the other hand, the thermally distributed carriers can be directly trapped into the surface states, contributing to the emissions with long wavelength. These irradiative states play dominating roles under different excitations and result in the fluctuation of PL intensities or the so called excitation dependent luminescence (Figure 4b). Additionally, oxidized carbons are corresponding to the common green or longer wavelength light.

Compared with traditional organic dyes and semiconductor quantum dots, CDs and GQDs possess higher photostability and low photobleaching. The former enables long term real-time imaging while the latter permits single-molecule tracking. Carbon nanorings exhibit excellent fluorescent stability under the illumination of a UV lamp (365 nm, 20 W) for 16 h.[19] No distinct photobleaching was observed for GQDs prepared from solvothermal method using hand UV lamp or mercury (Hg) lamp with low power and decrease on PL intensity was only observed when using 1000 W high pressure Hg lamp.[57] The PL intensity of CDs prepared with laser ablation decreased only by 4.5% even after 4 h, whereas other organic materials such as polystyrene nanospheres photobleach within 0.5 h.[64] When measuring the fluorescence of GQDs at different ionic strengths (increase the concentration of KCl from 0 to 2.0 M), there were no changes in either the PL intensities or the peak sites, indicating the high photostability in biological tissues and possible applications in biology.[57]

3. Multiple Applications of CDs and GQDs

3.1. Light Emitting Diodes

As new kinds of luminescent materials, CDs and GQDs are expected to replace phosphors in white light emitting diodes (WLEDs) with rear earth metals and toxic elements such as cadmium and lead because of their low cost, high quantum yield (QY), high stability and low toxicity. Consequently, some efforts have been paid to fulfill the applications of CDs and GQDs in LEDs. They can work both as phosphors in WLEDs or active layers in electroluminescent devices.

3.1.1. Phosphor Based WLEDs

The popularization of WLEDs can save a lot of electricity. However, traditional WLEDs with rear earth metals or toxic elements are undergoing the issues about cost and stability. Then, researchers are exploring new materials to decrease the cost and increase the stability and luminescent carbon materials are claimed to be potential materials. Chen et al. prepared CDs with broad yellow fluorescence by a one-step pyrolysis from *N*-acetylcysteine and white light-emitting diodes were fabricated by combining the yellow emitted CDs with blue GaN-based LED chips (the peak wavelength centered at 460 nm).[65] The as-prepared WLEDs exhibit white light with CIE coordinates of (0.34, 0.35), which is very close to the balanced white light emission (**Figure 5**a). Commonly, the strongest emission of CDs is centered at blue region and the corresponding excitation wavelength is centered at UV region. To make the best of the fluorescence, researchers fabricated WLEDs with UV light LED chips. For example, Guo et al. fabricated WLEDs with UV LEDs (the peak wavelength centered at 360 nm) and CDs prepared by unzipping photonic crystals (Figure 5b). Though warm light with color coordinates of (0.45, 0.44) was obtained, the inevitable leak of UV light is not environmentally friendly.[66–68]

To fabricate phosphor based WLEDs, solid films are necessary. However, aggregation induced quenching (AIQ) effect inhibited the development and applications of CDs and GQDs greatly. To avoid this effect, Qu group prepared solid-state and luminescent CDs/starch composites with high quantum yield innovatively.[20] WLEDs at an optimized current of 50 mA (2.8 V), and a cool white light with CIE coordinates of

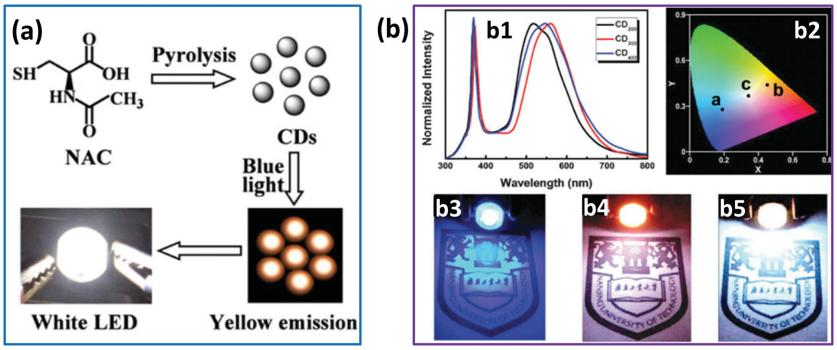

Figure 5. Recent progresses on photo-pumped LED applications of CDs and GQDs. a) Schematic of the formation of CDs from *N*-acetylcysteine and application in white LEDs. Reprinted with permission.[65] Copyright 2013, Springer. b) Emission spectra, CIE 1931 chromaticity chart and Photographs of the corresponding LEDs. Reprinted with permission.[66] Copyright 2012, Royal Society of Chemistry.

(0.26, 0.33) were obtained. For CDs, there are usually various surface groups, which act as electron donors and acceptors. The interaction between different surface states during drying samples can facilitate the AIQ behavior, which is similar to organic fluorescent dyes.[69] Considering the AIQ effect of surface states on the luminescence, we designed and achieved carbon nanorings with relatively pure surface. The donor–acceptor attraction among adjacent luminescent carbon nanounits would be greatly depressed, and hence luminescence in the solid state could be persisted. Fortunately, WLEDs fabricated with these luminescent carbon nanorings exhibited CIE coordinates of (0.27, 0.28).[19] Kown and co-workers developed a method to fabricate CDs and GQDs in oil phase, which was suitable to fabricate CDs/Polymethyl methacrylate (PMMA) composites with excellent optical properties.[18,70,71] Applying a current of 50 mA (≈3 V, optimized), WLEDs based on the InGaN blue LED (400 nm) exhibited cool white light with CIE coordinates of (0.37, 0.45) and correlated color temperature (CCT) of 5080.4 K. Additionally, luminous efficacy of 108.19 lm W_{opt}^{-1} and high emission stability over 12 h was obtained.

3.1.2. Electroluminescence

Except for phosphor based LEDs, researches about applications of CDs and GQDs in electroluminescence are glowing recently, beginning with the fabrication of OLED device based on GQDs (as shown in **Figure 6**a).[16] Mixtures of poly(2-methoxy-5-(2-ethylhexyloxy)-1,4-phenylenevinylene) (MEH-PPV) and methylene blue functionalized GQDs (MB-GQDs) were employed as the light emitting layer. The turn on voltage decreased from 6 V for pure MEH-PPV to 4 V for MEH-PPV with 1% MB-GQDs. A higher concentration of MB-GQDs resulted in charge trapping as well as a shortening effect because of agglomeration. The additional electrical transport paths after the introduction of GQDs lead to high efficiency charge injection and then enhanced internal quantum efficiency. Before long, WLEDs based on CDs' electroluminescence were fabricated without any functionalization or addition (Figure 6b1).[22] poly(3,4-ethylenedioxythiophene) : poly(styrenesulfonate) (PEDOT : PSS) was used as a buffer layer on the anode in order to increase the work function of ITO and to reduce the surface roughness of the anode (Figure 6b2,b3).[72] 1,3,5-tris(*N*-phenylbenzimidazol-2-yl) benzene (TPBI) was used as the electron transport layer and 1 nm thick LiF and 120 nm thick Al were used as electrodes. An external quantum efficiency of 0.083% at a current density of 5 mA cm^{-2} was realized. The corresponding CIE coordinates are (0.40, 0.43), with a color-rendering index (CRI) of 82. Though the efficiency of these works is still low, they open a window for the researches in electroluminescence, indicating the possibility of making LEDs with CDs and GQDs.

More interesting works are reported recently. Kwon et al. prepared GQDs with controllable size by an amidative cutting method.[21] The size of the GQDs can be tuned by simply regulating the amine concentration used in synthesis. The energy gaps of the GQDs are tuned via varying the size, exhibiting colorful PL ranging from blue to brown. Finally, OLEDs were prepared with 4,4′-bis(carbazol-9-yl) biphenyl (CBP) as a host and GQDs as a dopant, as shown in Figure 6c1. The energy levels are placed inside those of CBP and the sample with an active layer thickness of 10 nm shows the brightest white electroluminescence (Figure 6c2,c3). An efficiency of 0.1% was obtained, which is the best result up to date for GQDs based LEDs. However, such efficiency is quite lower than that of the state of the art OLEDs or quantum dot based LEDs in spite of the improvement compared with previous reports.[73,74] CDs are also employed as the active materials for the application of LEDs with a similar method (Figure 6d1). Color switchable electroluminescence was observed under different working voltages, ranging from blue to white (Figure 6d2,d3).[75] This interesting phenomenon may originate from the abundant irradiative decay states related to surface groups and defects. At low voltage, carriers will be injected into the shallow energy state with short lifetime, consistent with fast decay of excited charges. Therefore, when ZnO is used as the electron transport layer, high current injection can be realized, leading to white light emission with a luminance of 90 cd m^{-2}.

In addition, other efforts have also been paid to realize the application of GQDs or CDs in electroluminescence devices.[47,76] However, the efficiency is still too low to be used in commercial devices. Both material characterizations and device structures are needed to be designed carefully from the aspect of practical applications.

3.2. Photodetectors

As a reverse process of electroluminescence, photo-generated carriers can be collected and used in various devices, such as photodetectors (PDs), solar cells, photocatalysis and so on. Actually, as excellent optical materials with high absorption and luminescence, it is easy and merited for us to think of their applications for optoelectronic devices. But, it is different from photoluminescence because good electrical conductivity is essential for devices. However, most of the CDs and GQDs possess poor crystallinity

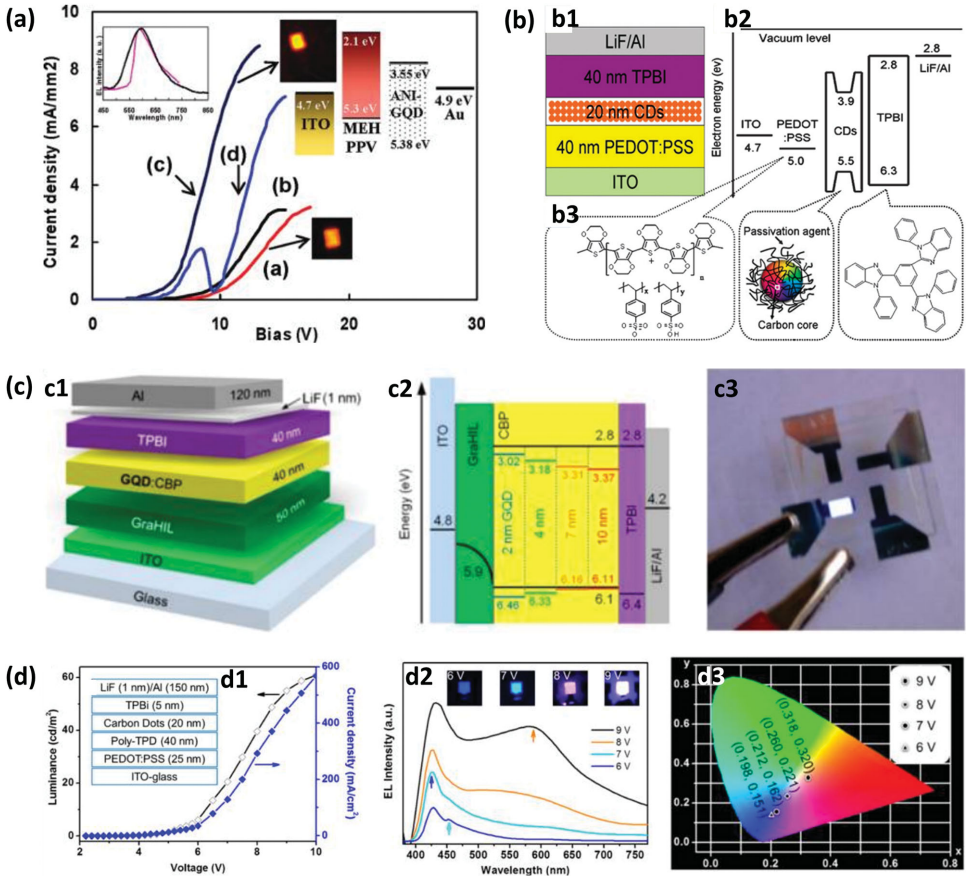

Figure 6. Recent progresses on electri-pumped LED applications of CDs and GQDs. a) Measured current density of MEH-PPV with different concentrations of MB-GQDs as a function of the applied voltage. Reprinted with permission.[16] Copyright 2011, American Chemical Society. b1) Schematic diagrams of the WLED. b2) Energy band diagram of the WLED relative to ITO and LiF/Al work functions. b3) Molecular structures of PEDOT : PSS and TPBI, and the schematic drawing of the CDs. Reprinted with permission.[22] Copyright 2011, Royal Society of Chemistry. c1) Physical and (c2) electronic structures of OLEDs employing the doped GQDs. c3) Digital image of white light emission from above GQDs based OLED. Reprinted with permission.[21] Copyright 2014, American Chemical Society. d1) Current density and Luminescence of the CDs based LED. d2) Electroluminescence spectra and digital photographs of blue, cyan, magenta, and white emissions. d3) CIE coordinates of the CDs based LED operated under different voltages. Reprinted with permission.[75] Copyright 2013, American Chemical Society.

compared to inorganic quantum dots, resulting in worse conductivity. Therefore, it is relatively difficult to prepare devices with CDs and GQDs. Researchers have designed and fabricated various devices and next, we are going to introduce these photoelectronic devices associated with GQDs and CDs.

First of all, we will demonstrate the applications in photodetectors. Response band and responsivity are basic parameters for PDs. Commonly, the absorption peak at ≈250 nm of CDs and GQDs is attributed to the π–π^* transition, which is in the deep-UV region. Therefore, deep-UV photoluminescence[47] and photodetection is possible for CDs and GQDs.[24] For example, Tang et al. prepared nitrogen doped GQDs with broad emission spectra ranging from 300 to 1000 nm using glucose and aqueous ammonia. Photodetectors with responsivity as high as 325 V/W were fabricated by a simple drop-coating method on interdigital gold electrodes (**Figure 7**a1).[77] The broadband emissions are claimed to originate from the layered structure of the GQDs which create a large conjugated system containing extensive delocalized π electrons. Interestingly, the GQDs based photodetectors exhibit negative photocurrent when irradiated with different light, which can be explained as following. Because of the surface passivation of GQDs, photogenerated electron-hole pairs cannot move freely (Figure 7a2,a3). The bound excitons may trap carriers when exposed to light, forming photoinduced charge traps. And then, carriers will be trapped when they pass through the GQDs, leading to the negative photoresponse. Kim and co-workers also fabricated GQDs based PDs with high detectivity (higher than 10^{11} cm $Hz^{1/2}$ W^{-1}), high responsivity (0.5 A W^{-1}) and broad spectral range (from UV to infrared).[78] Figure 7b1 shows the sandwich structure between slightly p-type graphene sheets of the device. The dark *I*–*V* curve of the device shows asymmetric and nonlinear properties with varying bias voltage because of tunneling through the available density of states of GQDs between graphene sheets. Such phenomenon can be explained according to the band structure shown in Figure 7b2-b4 that when a forward bias is applied, a current will flow if the bias voltage exceeds the energy between the Fermi level of bottom graphene and the lowest unoccupied molecular orbital (LUMO) of the GQDs. It is suggested that both the photoexcited electrons and holes and carriers multiplication by

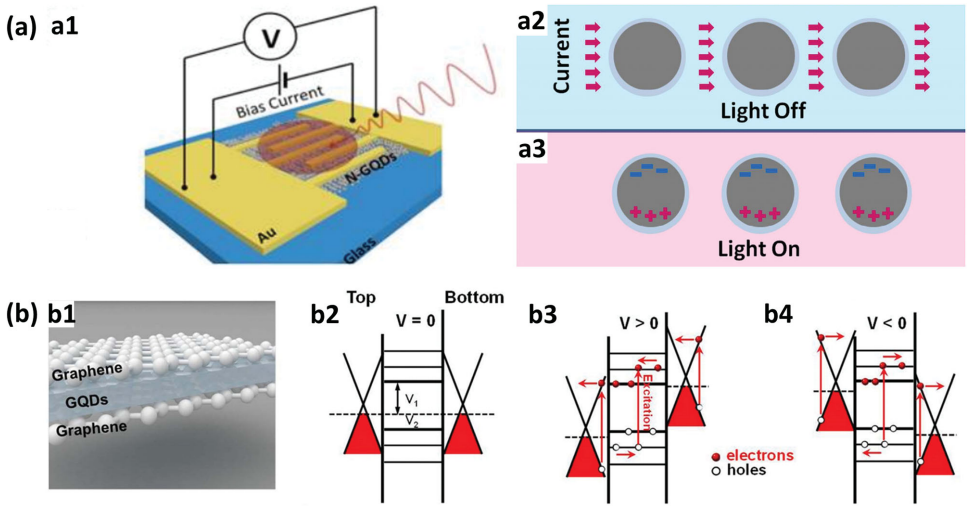

Figure 7. Recent progresses on photodetector applications of CDs and GQDs. a1) Schematic diagram of the GQDs photodetector. The unusual negative photoresponse mechanism of the GQDs photodetector (a2) light off, a3) light on). Reprinted with permission.[77] Copyright 2014, American Chemical Society. b1) Schematics of a GQDs PD device and band diagrams under b2) no, b3) forward, and b4) reverse biases. Reprinted with permission.[78] Copyright 2014, Nature Publication group.

impact ionization contribute to the enhancement of photocurrent. The high gain results from the long lifetime of carriers and short transit time from GQDs to graphene sheets.

In addition to the direct use of CDs or GQDs in PDs, elaborate design of device structure and band alignment can also make PDs benefit from the usage of CDs and GQDs. For instance, Xie et al. fabricated silicon nanowire arrays/CDs core-shell heterojunction PDs with a wide spectra region, high responsivity (353 mA W^{-1}) and fast response speed (rise time = 20 µs, fall time = 40 µs), as shown in **Figure 8**a1. The enhanced performances benefit from effective suppression of recombination and enhanced optical absorption. As shown in Figure 8a2, the LUMO energy of CDs is ≈2.26 eV, which is much higher than the conduction band of Si, resulting in a large barrier for the transport of electrons. The CDs film acts as an electron blocking layer that confines electrons in Si nanowires to suppress the recombination. With regarding to the transport of carriers, when Au or Ag is used as single kind of electrode, large barriers for hole and electron transportation will exist at the cathode or anode, because of the high and low work function of Au (5.1 eV) and Ag (4.26 eV) (Figure 8b1–b3), respectively. According to above analysis, Zhang et al. fabricate deep UV GQDs based PDs with asymmetric electrodes combined with Au and Ag, shown in Figure 8b4 and b5.[24] Ag serves as cathode while Au serves as anode. Thus, photogenerated carriers can drift freely toward electrodes under forward bias and carrier recombination can be suppressed because electrons and holes can be separated readily. The as prepared device possesses high on/off ratio even under a weak light of 8 µW cm^{-2} and the rise time and decay time are reduced to 64 and 43 ms, respectively.

3.3. Solar Cells

Another common kind of photovoltaic devices, which are similar to photodetectors, are solar cells (SCs), which depend on the use efficiency of photogenerated carriers. Besides, CDs and GQDs usually possess wide rang absorption with a tail extending to visible region,[63] which is beneficial for the application of solar energy. Up to now, many kinds of SCs have been reported, such as silicon based SCs,[23] organic SCs,[79,80] dye (dot)-sensitized SCs (DSSCs)[17,81] and so on.[63,82,83] The CDs and GQDs can play different roles of photo absorption agents, sensitizers and transporting layers and the efficiency varied from 0.1 to 9%. In this section, we are going to talk about the applications of CDs and GQDs in photovoltaic devices according to the materials used.

The high conversion efficiency of silicon based SCs contributes to their wide applicarions. For example, CDs/silicon nanowire arrays core-shell devices were fabricated, as discussed above. Because of enhanced absorption and suppressed recombination, the devices get a conversion efficiency of 9.1%, which is comparable to that of Si based hybrid SCs.[84] Similar structure is also employed by Gao et al. and a conversion efficiency of 6.63% is obtained, as shown in **Figure 9**a1,a2. Such improved performance compared to bare Si or graphene oxide hybrids can be explained by the special energy band structure of GQDs, which behave as an electron blocking layer.[14] Interestingly, the size of GQDs plays an important role that open-circuit voltage (V_{OC}) of the device increases while short-circuit current (J_{SC}) deceases with the decrease of size. The quantum size effect accounts for this phenomenon that the heterojunction barrier increases with the decrease of size and the barrier for hole transportation increases, resulting in the increase of V_{OC} and decrease of J_{SC}, respectively. In fact, to make the best of the photogenerated carriers, many approaches have been applied to facilitate the separation and to suppress the recombination of carriers. The interfaces between materials, layers and different units are very important for the enhancement of SCs. For example, ZnO nanorod arrays decorated with CDs or GQDs are prepared (Figure 9b1).[82,85] The band alignment of the device is shown in Figure 9b2 that electron transfer is quite

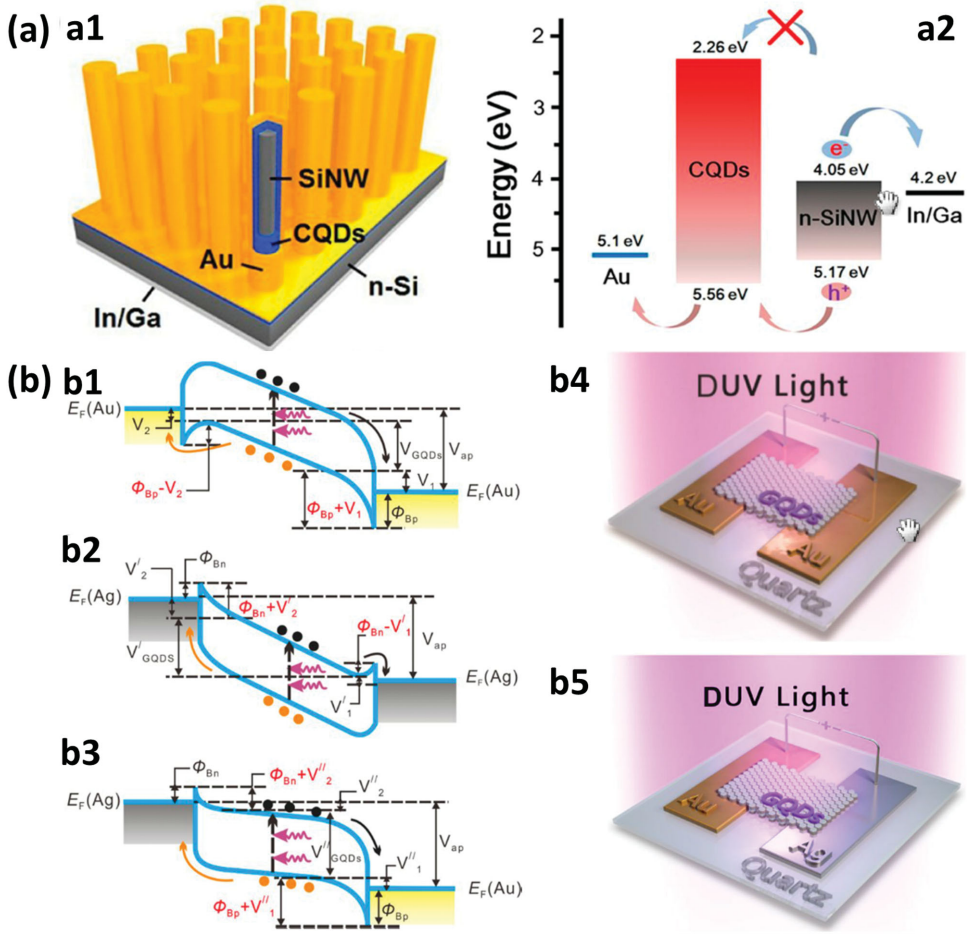

Figure 8. Recent progresses on photodetector applications of CDs and GQDs. a1) Structure of the Si nanowire arrays/CDs heterojunction device. a2) Energy band diagram of the Si nanowire arrays/CDs heterojunction. Reprinted with permission.[23] Copyright 2014, American Chemical Society. b) Energy band diagrams of GQDs based PDs with b1) Au–Au, b2) Ag–Ag, and b3) Ag–Au electrodes, respectively. Illustration of the GQDs based PDs with b4) symmetric and b5) asymmetric electrodes. Reprinted with permission.[24] Copyright 2015, American Chemical Society.

feasible at the interface of GQDs and ZnO arrays. Besides that, other kinds of solid-state solar cells are also fabricated, combining inorganic quantum dots and CDs.[17,86] It turns out that facilitation of the charge propagation from CDs and Förster resonance energy transfer improve the device performance greatly.

All solutions processed organic and dye sensitized solar cells have attracted much attention because of their low cost, large area, random substrate and facile and scalable engineering such as spin-coating, inject printing and roll-to-roll methods. These devices can also benefit from the broad absorption, special band structure and electron transportation ability of CDs and GQDs. Li and co-workers fabricated a bulk heterojunction (BHJ) organic solar cell based on an composite layer of poly(3-hexylthiophene) (P3HT) and GQDs (**Figure 10**a1).[42] We can see that the LUMO energy level of GQDs is in the range of 4.2–4.4 eV, which is just between the LUMO of P3HT and the work function of Al (Figure 10a2), forming an electron transport cascade. This band structure will facilitate the dissociation of excitons and good crystallinity of GQDs will improve the charge transport through the active layer. Thus, a photo conversion efficiency of 1.28% was obtained and such structure without C60 was accepted by other groups to fabricate organic solar cells.[16,18] High V_{OC} (1.6 V) and conversion efficiency about 1% can be obtained. Though the efficiency of these devices is still low compared to conventional organic solar cells, it is expected that GQDs or CDs can be promising alternatives to the expensive C60 as electron acceptors.

DSSC is another kind of photovoltaic device that utilizes dyes to absorb sun light. GQDs with maximum absorbance at 591 nm and high molar extinction coefficient of 10^5 M^{-1} cm^{-1} (about an order of magnitude higher than that of commonly used metal complexes) were first applied in DSSCs by Yan and co-workers.[15] However, limited efficiency is obtained, with a rather low short current density of 200 μA cm^{-2} because of the weak affinity of GQDs and TiO_2 surface. Such physical adsorption is detrimental to the charge injection that functionalization for covalent attaching and adjusting of band energy structure are highly sought. Device with the same configuration was fabricated by employing nitrogen doped CDs (NCDs) as shown in Figure 10b1.[81] In situ hybridization of TiO_2 with CDs and lowered work function induced by nitrogen doping contribute to the improvement of device performance (Figure 10b2). A V_{OC} of 0.46 V and a J_{SC} of 0.69 mA cm^{-2} was obtained, with a conversion efficiency of 0.13%. Recently, DSSCs combined with dyes

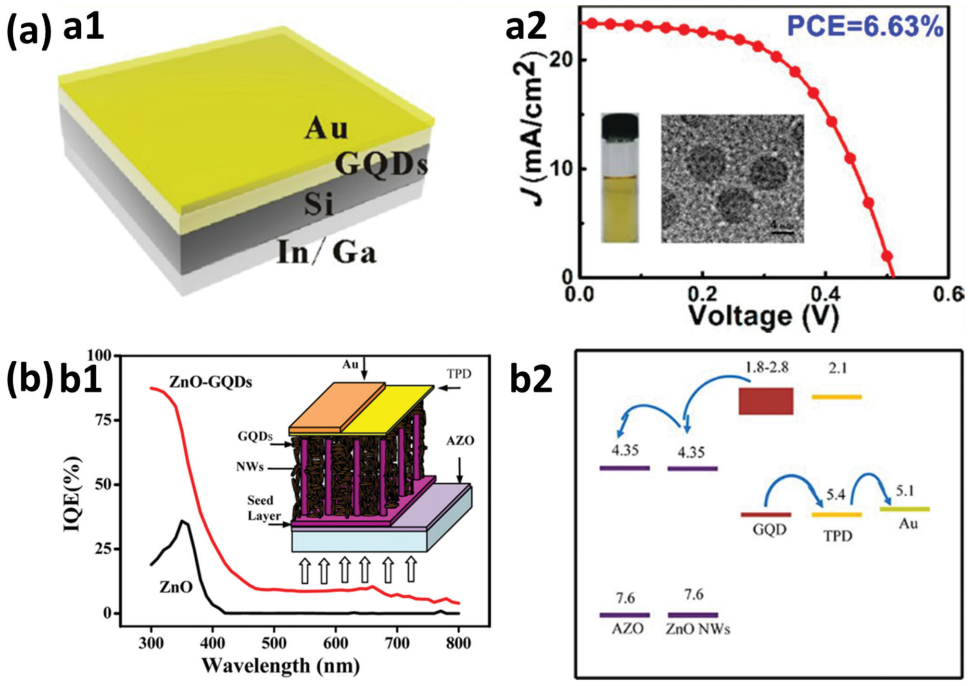

Figure 9. Recent progresses on solar cell applications of CDs and GQDs. a1) Illustration of the crystalline Si/GQDs heterojunction solar cell. a2) *J–V* curve of the Solar cell. Reprinted with permission.[14] Copyright 2014, American Chemical Society. b1) Internal quantum efficiency of the samples. The inset shows the structure of the device. b2) Band diagram of the device. Reprinted with permission.[82] Copyright 2012, American Chemical Society.

and GQDs (co-sensitizers) were fabricated and high conversion efficiency was achieved.[87,88] A type II alignment for TiO_2/GQDs/dye configuration was realized by tuning electronic levels of GQDs and such cascaded alignment of energy levels enhances the charge separation and collection. Additionally, energy transfer from GQDs to dyes because of the overlap between the PL of GQDs and absorption of dye promotes the application of solar energy. Last but not the least, electron recombination to the redox couple is reduced because of the inhibition of the back electron transfer to the electrolyte by the GQDs. Therefore, DSSCs exhibit an efficiency of 6.1%, higher than that of device without GQDs by 19.6%.

Organic/inorganic hybrid solar cells combined with metal oxides and organic semiconductors have also achieved researchers' attention while it remains challenges to match the energy levels of the donor–acceptor system. Qin et al. demonstrated the insertion of GQDs in organic/inorganic layers or combination with organic semiconductors, which led to an enhancement of the power conversion efficiency.[80,83] As shown in Figure 10c1, a cascaded alignment of energy levels similar to that of above discussed devices is obtained, facilitating the separation of photogenerated carriers. On the other hand, most of the applied oxides and organics can only absorb the solar energy partially and the insertion of GQDs with broad absorption spectra enhances the harvest of incident light. All of these factors contribute to the performance of solar cells (Figure 10c2).

3.4. Photocatalysis

Human activities have led to myriad wastewater containing toxic matters such as heavy metal ions and organic compounds, which are difficult to be removed. Besides, worsening environment desires the application of clean energy such as hydrogen. For commercial aims, highly efficient catalysts with low cost are in deadly demand to replace expensive metals such as Pt. All of them can benefit from CDs or GQDs according to the reports. TiO_2 is considered as the most promising photocatalyst. However, the wide band gap (in the UV region) inhibits the total utilization of solar energy because visible and infrared parts account for the majority. To make the best of the solar light, different TiO_2 nanostructures (nanoparticles and nanowires) decorated with CDs and GQDs are fabricated.[35,43,89] On one hand, CDs and GQDs can absorb broader band beyond UV light, increasing the use of incident light. On the other hand, type II band structure ensures efficient separation of carriers and crystalline oxides provide good transport channels for carriers. Regarding with these factors, improved photocatalysis of organic compounds such as methylene blue (MB) is observed even under visible light.

Photocatalytic water-splitting into H_2 and O_2 using solar energy has attracted considerable attention as a renewable energy resource and much work has been done with CDs and GQDs.[90–92] However, present photocatalysts still suffer from low efficiency and poor stability. Recently, Kang group fabricated CDs/C_3N_4 composites, which exhibited excellent water splitting under visible light. The highest quantum efficiency of 16% is obtained and an overall solar energy conversion efficiency reach to 2.0%.[25] **Figure 11**a1 shows the reaction mechanism of visible light water splitting by CDs/C_3N_4 composites. A two-electron, two-step pathway dominates the generation of H_2 that C_3N_4 is responsible for the first step and CDs are in charge of the second step. Additionally, CDs also increase the

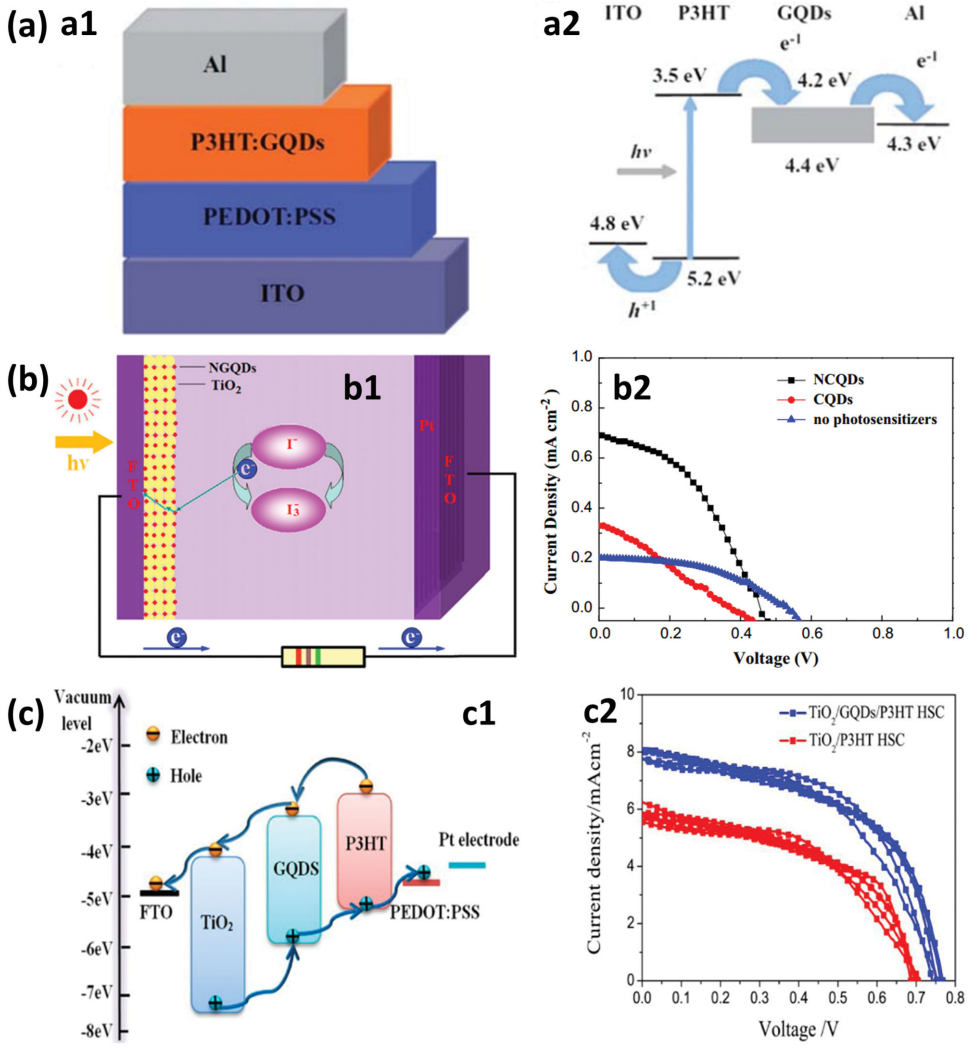

Figure 10. Recent progresses on solar cell applications of CDs and GQDs. a1) Schematic and a2) energy band diagram of the GQDs based organic solar cell. Reprinted with permission.[42] Copyright 2011, Wiley-VCH. b1) Schematic device structure of GDQs based dye-sensitized solar cell. b2) Current–voltage curves of the devices with and without GQDs. Reprinted with permission.[81] Copyright 2013, Elsevier. c1) Energy band diagram of organic/inorganic hybrid solar cell. c2) *C–V* curves with and without GQDs. Reprinted with permission.[83] Copyright 2015, American Chemical Society.

light absorbance and the wavelength dependent quantum efficiency is consistent with the absorbance spectrum. The synergetic effect of C_3N_4 and CDs (appropriate band structure, high porous structure for C_3N_4, high stability and low cost) make the composites promising photocatalyst for visible light-driven water splitting. Yeh et al. report the application of nitrogen doped GQDs for overall water-splitting under visible light.[91] The nitrogen doped GQDs possess a band-gap of 2.2 eV, which is favorable for the absorbing of visible light. Most interestingly, nitrogen atoms in the graphene frame result in n-type conductivity while grafted oxidized groups on the surface cause p-type conductivity, as shown in Figure 11b1. It means that quasi in situ p-n junction is realized in confined regions and sp^2 clusters serve as the junction with Ohmic contact. The p- and n-domains are responsible for the production of H_2 and O_2, respectively, which can be confirmed by the results of separate evolution of H_2 and O_2 (Figure 11b2,b3). Such metal free catalyst provides sustainable and environmentally friendly strategy for water splitting under visible light. CDs modified TiO_2 (P25) composites are also prepared with a facile hydrothermal method, which exhibit a H_2 evolution rate of 4 times higher than that of P25 after optimization.[90]

If wastes can be transformed into fuels and valuable chemicals with low cost and sustainable approaches, there will be incredible changes through the whole world. In addition, industrial catalysts possessing high catalytic efficiency but without expensive metals are favorable for the decrease of cost. CDs/Cu_2O heterostructures are fabricated for the conversion from CO_2 to methanol with solar light by Li and co-workers. Cu_2O microspheres decorated with CDs of ≈5 nm create multiple reflections of light between protruding particles, which enhance the absorption of sunlight, resulting in stronger photocatalytic activity, as shown in Figure 11c1. The reaction rate can also be affected by the loading mass of CDs and the highest reduction rate of 55.7 μmol g^{-1} h^{-1} from CO_2 to methanol is obtained. The excellent cayalytic activity is also attributed to the

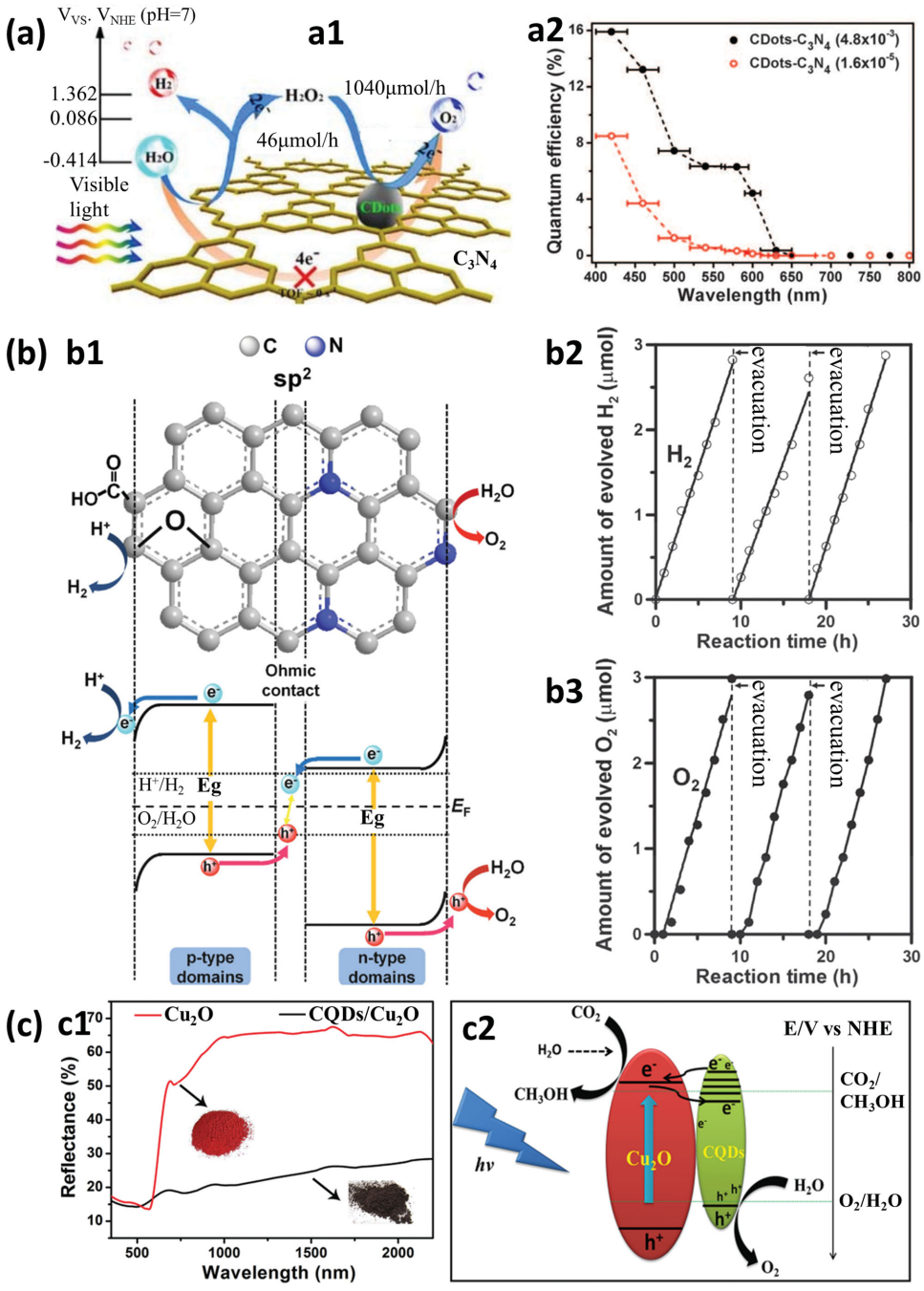

Figure 11. Recent progresses on photocatalysis applications of CDs and GQDs. a1) Reaction mechanism for visible light water splitting by CDs/C_3N_4 composites. a2) Quantum efficiency of water splitting under various wavelengths and with two different concentrations. Reprinted with permission.[25] Copyright 2015, AAAS. b1) The configuration and energy diagram for the GQD photochemical diode consists of the p- and n-type domains, connected through the sp^2 clusters as Ohmic contact. Evolution of b2) H_2 and b3) O_2 over 1.2 g of GQDs. Reprinted with permission.[91] Copyright 2014, Wiley-VCH. c1) Diffuse reflectance spectroscopy reflectance of CDs/Cu_2O and Cu_2O (the inset shows the model of enhanced absorption by CDs/Cu_2O. c2) Schematic of the proposed photocatalytic mechanism of CO_2 reduction catalyzed by CDs/Cu_2O. Reprinted with permission.[93] Copyright 2015, Wiley-VCH.

good charge separation (Figure 11c2) at interfaces and transfer capabilities of the CDs. Synthesis of metal nanoparticle/CDs composites for cyclohexane oxidation with high efficiency and selectivity has also been reported.[94] Especially, the Au/CDs composites exhibit 63.8% conversion efficiency and 99.9% selectivity for the green oxidation of cyclohexane to cyclohexanone under visible light irradiation and room temperature. Synergic effect of surface plasma resonance and interaction between metal particles and CDs contributes to the excellent photocatalytic activities.

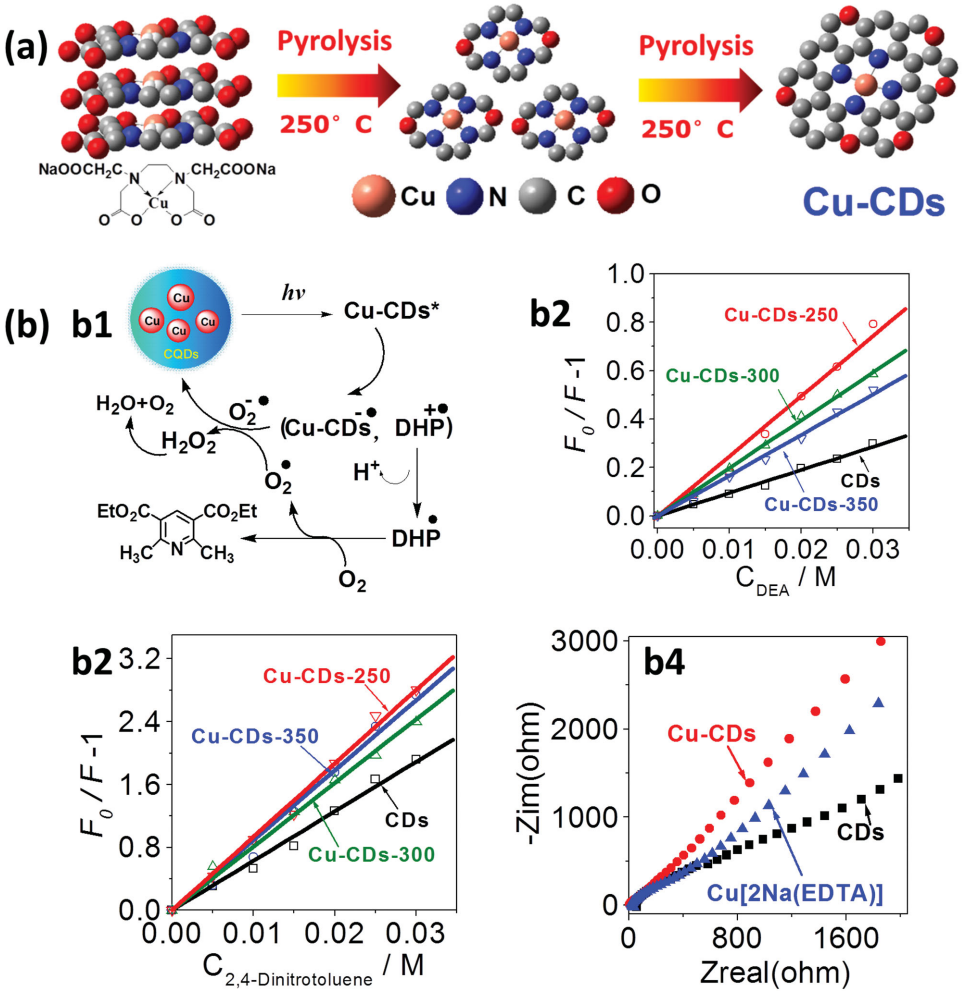

Figure 12. Recent progresses on photocatalysis applications of CDs and GQDs. a) Fabrication and pyrolysis reaction procedures of Cu/N-CDs. b1) Photooxidation mechanism of CDs. Stern-Volmer plot of the emission intensity of CDs with various amounts of b2) DEA and b3) 2,4-dinitrotoluene upon excitation at 350 nm in H_2O. b4) Nyquist diagrams of different CD samples. Reprinted with permission.[95] Copyright 2015, Wiley-VCH.

In addition to the fabrication of composites for the enhancement of photocatalysis, improving the electrical and optical properties of the material itself is just equally important. However, photocatalysis applications are being impeded by the poor electron transfer inside CDs. Recently, Wu et al. reported on the synthesis of Cu–N doped CDs (Cu/N-CDs) through one-step pyrolytic synthesis of CDs with Cu[2Na(EDTA)] (**Figure 12**a).[95] Cu species chelate with carbon matrix through Cu–N complexes. Figure 12b1 shows the photooxidation mechanism of 1–4 DHP. After excitation, electrons transfer from 1,4-DHP to CDs, forming highly reactive 1–4 DHP^+. H^+ is released and electron transfer process from 1,4-DHP$^•$ to O_2 results in the production of aromatization product and reactive oxygen radical. $O_2^{•}$ grabs electron from CDs and the catalyst recovers. At the same time, superoxide anion radical is produced and reacts with H^+ and then H_2O_2 are generated, which will decompose into H_2O and O_2 as a green route. The quenching effect of emission intensity by well-known electron acceptor 2,4-dinitrotoluene and electron donor *N*,*N*-diethylaniline (DEA) were measured (Figure 12b2,b3) to study the electron accepting and donating abilities of CDs, which were enhanced 2.5 and 1.5 times because of the co-doping of N and Cu. The electronic conductivity of Cu/N-CDs increases to 171.8 μs cm^{-1} (Figure b4). As a result, the photocatalysis efficiency in the photooxidation reaction of 1,4-DHP is improved 3.5 times compared to common CDs.

3.5. Energy Related Applications

With the increasing concerns regarding environmental issues caused by the consumption of fossil-fuel and rapid depletion of non-renewable resources, people are seeking clean and renewable energy resources, such as solar energy,[96–98] wind energy and water conservancy. However, these methods provide discrete energy, which will influence the work of the grid. Therefore, energy storage, a key component in the energy conversion, storage and delivery chain, has atracted worldwide attentions.[99] In addition, fast development of hybrid vehicle and portable electronics require further improvement of energy storage devices beyond traditional carbon based devices. Up to date, many kinds of oxides,[100,101] sulfides[102] and elementary

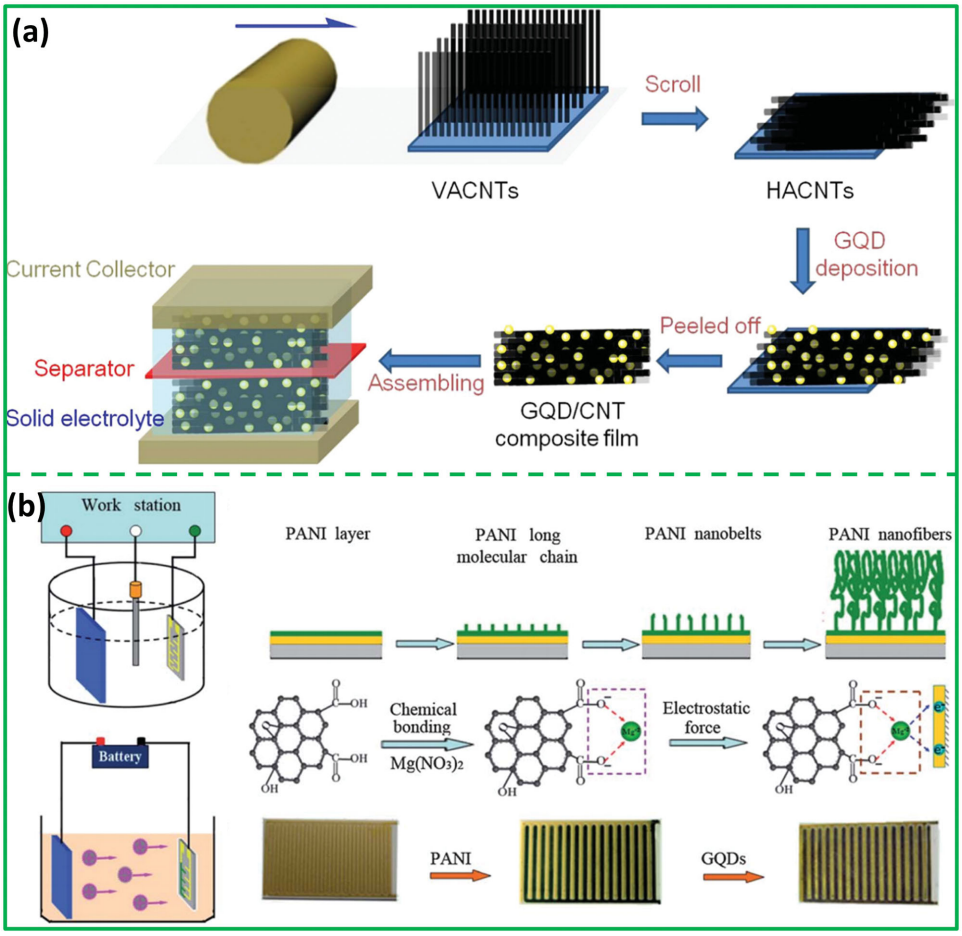

Figure 13. Recent progresses on supercapacitor applications of CDs and GQDs. a) Schematic of the preparation of a symmetric supercapacitor based on GQDs/carbon nanotubes. Reprinted with permission.[105] Copyright 2013, Springer. b) Schematic of the electrochemical deposition of PANI nanofibers, GQDs, and the structure of the device. Reprinted with permission.[106] Copyright 2013, Royal Society of Chemistry.

substance[103,104] were used to fabricate energy storage devices, such as lithium ion batteries and supercapacitors. The former benefit from high energy density and the latter possess high power density. Both of them are necessary for the practical applications.

3.5.1. Supercapacitors

Supercapacitors and batteries are reported to benefit from GQDs and CDs. Principally, there are two kinds of supercapacitors according to the charge storage mechanism, double layer capacitors (ion absorption) and pseudocapacitors (Faradaic reaction), respectively. Hu et al. deposited GQDs onto aligned carbon nanotubes by an electrical method.[105] The preparation process and fabrication of the devices are shown in **Figure 13**a. A capacitance of 44 mF cm^{-2} was obtained, exhibiting a more than 200% improvement over that of bare CNT electrodes, 14 mF cm^{-2}. Considering the formation of micropores between GQDs and HACNT scaffolds and neighboring GQDs, here, the authors referenced the electric double-cylinder capacitor (EDCC) model.[107] Such structure facilitated the amount and transportation of ions, resulting in high capacitance and stability. Similarly, GQDs and other carbon porous structures, such as graphene[108] and three dimensional aerogel,[109] are applied. At least 100% improvement is obtained in these works thanks to the high specific surface area and easy access and diffusion of ions.

Despite capacitors used in workplace with higher energy, micro-supercapacitors applied in portable electronics are studied. A GQDs based symmetric micro-supercapacitor was firstly prepared by Liu et al., using a simple electro-deposition method on interdigital gold electrodes.[110] The devices exhibited superior rate capability (1000 V s^{-1}) and excellent power response with very short relaxation time constant in both aqueous and ion liquid electrolytes. A capability of ≈97.8% of its initial specific capacitance after 5000 cycles was obtained, indicating the potential applications. Then, asymmetric device employing conductive polymer, polyaniline (PANI), was prepared with similar method, as shown in Figure 13b.[106] First of all, PANI nanofibers are prepared through an electrochemical method and then, GQDs are electrodeposited on aligned PANI fibers. Such devices employing PANI and GQDs as the positive and negative active materials also show high rate capability and short relaxation time constant of 115.9 ms.

Compared to double layer capacitors, pseudocapacitors associated with redox reactions usually exhibit higher energy density.

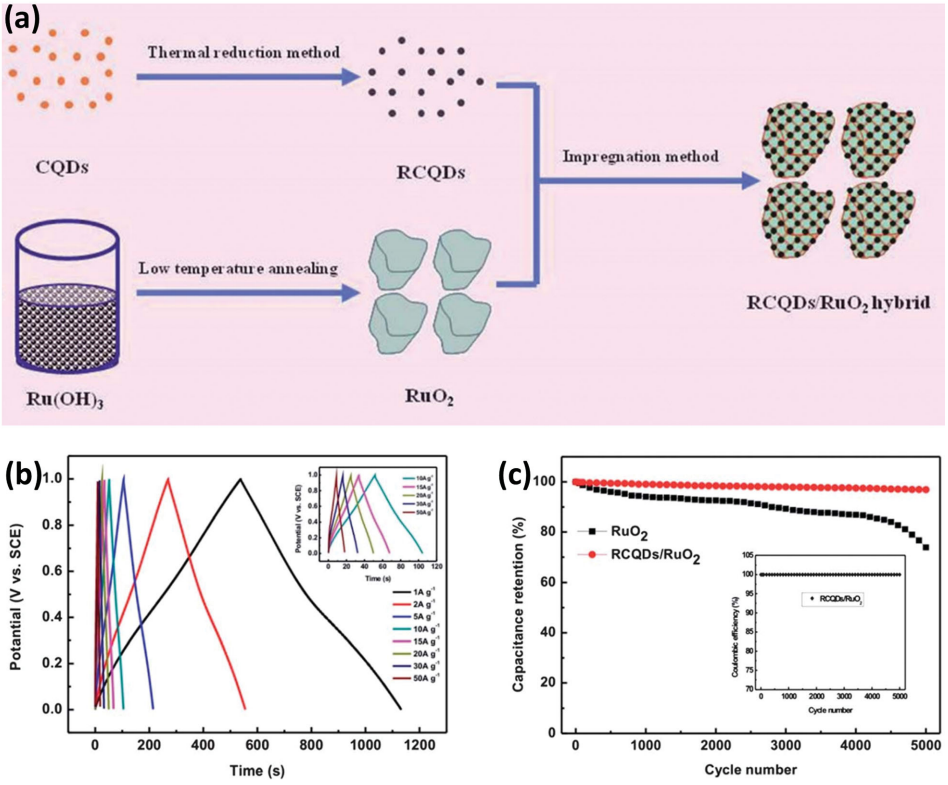

Figure 14. Recent progresses on supercapacitor applications of CDs and GQDs. a) Preparation procedure of CDs and RuO_2 networks. b) Charge and discharge curves under high current density (10–50 A g^{-1}). c) Cycling stability of the RuO_2 and CDs/RuO_2 at a current density of 5 A g^{-1}. Reprinted with permission.[27] Copyright 2013, Royal Society of Chemistry.

Obviously, higher specific surface area and more atoms participating in the redox reactions will result in higher specific capacitance. Zhu and co-workers prepared RuO_2 networks decorated with CDs with a simple method as shown in **Figure 14**a.[27] The introduction of CDs reduces the aggregation among RuO_2 nanoparticles, forming porous and multichannel structures. Electrodes measured in three-electrode system exhibit outstanding supercapacitances under ultrafast charge and discharge and excellent stability because of the enhancement of charge transport and ionic motion among the RuO_2 nanoparticles. It is worth noting that 96.9% of its initial capacitance and Coulombic efficiency of almost 100% are remained after 5000 cycles (Figure 14b,c). Besides, another route to enhance specific capacitance is to improve the conductivity of active materials. CDs after annealing possess better conductivity because of improved crystallinity, which will enhance the transport of electrons during particles, leading to improved rate capability. Such design is also applied in lithium ion batteries though researches are still rare.

3.5.2. Lithium Ion Batteries

Figure 15a shows the fabrication of CuO/Cu and CuO/Cu/GQDs nanowire composites.[111] Before this, there is no report on the application of GQDs in LIBs. Additionally, large volume expansion (174%), low electron conductivity (p-type semiconductor) and low initial Coulombic efficiency hinder the practical applications of CuO in LIBs. It is expected that the highly conductive copper and GQDs coating can decrease the electrochemical impedance and thus facilitate the transport kinetics. Considering these issues, Zhu et al. synthesized CuO/Cu/GQD tri-axial nanowire arrays successfully. Such soft protection of GQDs shows greatly increased surface conductivity and the stability of nanowire array structure. Compared to CuO/Cu composite structure, the tri-axial nanowire electrodes achieve high initial Coulombic efficiency (87%) and superior capability retention (high retention after 1000 cycles). The current collector, copper foam, also provides good conductivity for electrons because no binder is used. This method is suitable for the improvement of performance in other less-stable materials such as VO_2. GQDs coated VO_2 arrays were fabricated via similar method by the same research group as shown in Figure 15b1.[26] The effect of GQDs is similar with that in supercapacitors, separating VO_2 nanobelts from each other and avoiding the agglomeration as well as minimizing the dissolution of active materials, shown in Figure 15b2. Lithium ion batteries based on above electrodes exhibit a ≈99% initial Coulombic efficiency and 100% during the following cycles and 36% capacitor is retained when the current density increased from 1/3 C to 120 C. Incredibly, such structure delivers a retention of 94% of the original capacity after 1500 cycles at 60 C (Figure 15b3). Obviously, above results demonstrate a new approach to enhance the performance of battery electrodes, including lithium, sodium and other ion batteries.

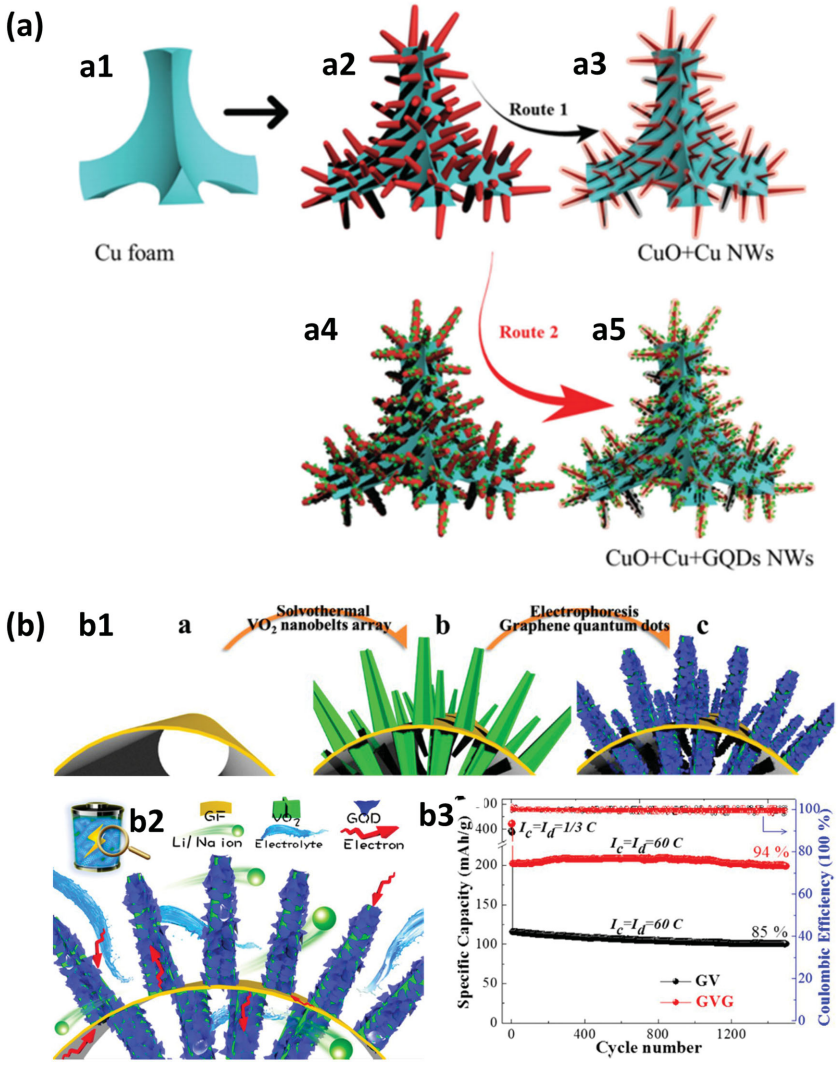

Figure 15. Recent progresses on battery applications of CDs and GQDs. a1–a3) Schematics of the fabrication process of CuO/Cu and a4,a5) CuO/Cu/GQDs nanowire electrodes. Reprinted with permission.[111] Copyright 2015, Wiley-VCH. b1) Fabrication processes of graphene frameworks supported VO_2 nanobelt arrays and coating of GQDs. b2,b3) Illustration of the electrode with multi-channels for the transfer of both electrons and ions. Reprinted with permission.[26] Copyright 2015, American Chemical Society.

Except for above discussed applications, GQDs and CDs are frequently reported to be employed in biological area because of its low toxicity, biocompatibility and high hydrophilicity, such as bioimaging in vivo or vitro[112] and drug delivery.[113] Another application for detection of toxic ions (Hg^{2+}) in water with high selectivity and sensitivity also attracts a lot of interest.[114] Interestingly, lasing emissions are observed for CDs in specific solvent and much more work and in-depth study should be carried out to understand the phenomenon.[115,116] Anyway, CDs and GQDs can unambiguously be used as the gain medium to achieve lasing.

4. Conclusions and Outlook

Figure 16 shows the timeline of the development in applications for CDs and GQDs. From the accidental discovery in 2004, researches have gone forward step by step till now and complex devices beyond photoluminescence have been fabricated, such as solar cells, LEDs, lithium ion batteries, supercapacitors, photodetectors etc. As discussed in this Feature Article, many kinds of devices and applications can benefit from CDs and GQDs because of their special optical and electrical properties. Elaborate designs of micro-structures and device structures in previous reports have provided promising strategies for practical applications and future researches. However, the research on CDs and GQDs is still at its early stage compared to graphene. There is still a long way to go for practical applications and there is also a large room for researchers.

First of all, there are still many issues waiting to be settled for further development. For instance, conclusive evidence and convincing explanation is still absent for the photoluminescence mechanism. How do the factors, such as crystallinity, size, surface functionalization and doping influence the optical properties is still unclear. Both in-depth experimental verification and theoretical calculations are deadly desired. Furthermore, scaled but facile synthetic methods for the production of CDs and GQDs with high quality are still challenges though many papers about fabrication methods have been published. All of the issues inhibit the development of this field.

Besides the fundamental researches, further development for applications is also important. For bioimaging in vivo and in vitro, long wavelength emission or up-conversion luminescence is more appropriate for biological window. However, QY is often low when excited with long wavelength light. Whilst, is it possible to combine photoluminescence and magnetism together for CDs and GQDs? It should have potential applications in biological diagnosis and treating. To realize this, doping of magnetic element or in situ combination of magnetic oxides such as Fe_3O_4 can be involved. New phenomenon and concept are also expected because of the interesting magnetism-photo interaction. Color rendering index (CRI), correlated color temperature (CCT) and Commission International de l'Eclairage (CIE) chromaticity coordinates are important parameters to evaluate the quality of white LEDs. However, up to now, most of the materials exhibit bright blue to green luminescence, high efficiency long wavelength emission is still absent to obtain WLEDs with high CRI, as well as warm white light. It is suggested that large sp^2 domain is favorable for yellow and red emission but the method is low efficiency.[49] Therefore, new methods for large scale production of CDs or GQDs with long emission wavelength are expected. Maybe doping of hetero atoms will also help such as electron donating atoms, which will enhance the conjugation degree, resulting in

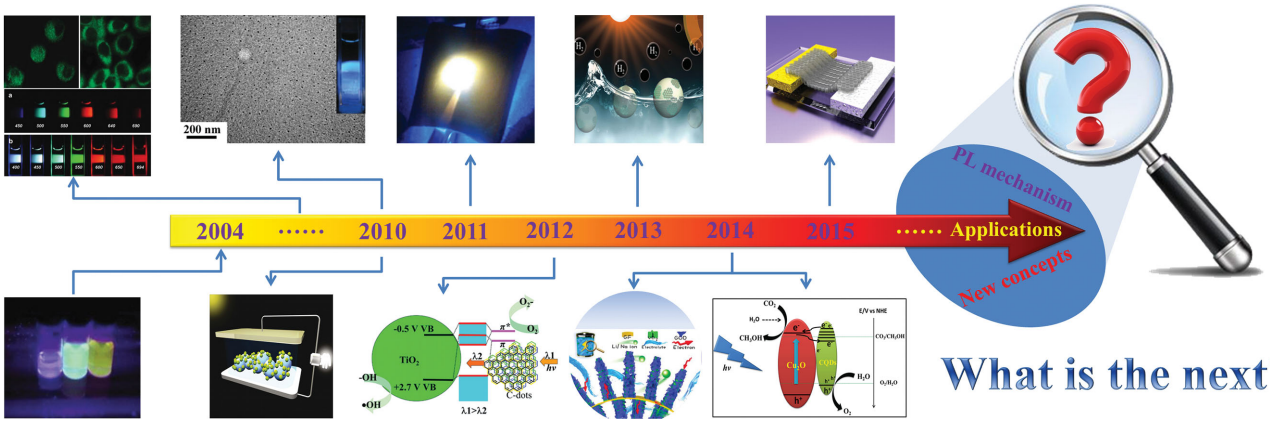

Figure 16. Timeline showing recent progress and future outlook on the applications of CDs and GQDs in communication- and energy-functional devices.[2,8,9,16,23,25,66,86,87,90] Reprinted with permission. Copyright 2004, 2006, 2013, 2015, American Chemical Society. Copyright 2010, 2015, Wiley-VCH. Copyright 2012, 2014, Royal Society of Chemistry.

narrower band gap. According to previous reports, electroluminescence is also possible for CDs and GQDs though quantum efficiency is still low and expensive organic semiconductors are used. It is still possible to improve device performance with less use of organics after the optimization of assembly and structure design. For energy storage devices, though these carbon materials can enhance the stability, post treatment is always needed to overcome the natural poor conductivity. Methods such as laser ablation in liquid that produce CDs with good conductivity and high yield can meet the demand.

Because of the high solubility, devices through all solution processed fabrication with large area and low cost is possible. Present techniques, such as roll-to-roll and dip coating methods can be employed to fabricate flexible and wearable devices with CDs and GQDs, including solar cells, photodetectors and LEDs. The technological process should be further improved for excellent assembly of films and materials' crystallinity and surface functionalization are also important for the tuning of electrical conductivity and forming of pinhole free films. Except for above discussed devices, CDs or GQDs with appropriate band gap and conductivity can compensate for the disadvantages of graphene to fabricate field effect transistors (FETs). Actually, FETs have been studied by Kwon et al. via solution method, effects of doping and ligand length on the performance of FETs are studied.[117] We are expecting more researches about FETs based on CDs and GQDs for electrochemical and biological sensing. In summary, we believe that new physical and chemical properties will be found and new applications and devices will be invented. They will be practically applied in some fields soon.

Acknowledgements

X.M.L. and M.C.R. contributed equally to this work. This work is financially supported by National Basic Research Program of China (grant number 2014CB931700), NSFC (grant number 61222403) and the Priority Academic Program Development of Jiangsu Higher Education Institutions.

Received: March 28, 2015
Revised: June 2, 2015
Published online: July 6, 2015

[1] K. S. Novoselov, A. K. Geim, S. V. Morozov, D. Jiang, Y. Zhang, S. V. Dubonos, I. V. Grigorieva, A. A. Firsov, *Science* **2004**, *306*, 666.
[2] X. Xu, R. Ray, Y. Gu, H. J. Ploehn, L. Gearheart, K. Raker, W. A. Scrivens, *J. Am. Chem. Soc.* **2004**, *126*, 12736.
[3] Y. Zhu, S. Murali, M. D. Stoller, K. J. Ganesh, W. Cai, P. J. Ferreira, A. Pirkle, R. M. Wallace, K. A. Cychosz, M. Thommes, D. Su, E. A. Stach, R. S. Ruoff, *Science* **2011**, *332*, 1537.
[4] E. Yoo, J. Kim, E. Hosono, H.-s. Zhou, T. Kudo, I. Honma, *Nano Lett.* **2008**, *8*, 2277.
[5] K. S. Kim, Y. Zhao, H. Jang, S. Y. Lee, J. M. Kim, K. S. Kim, J.-H. Ahn, P. Kim, J.-Y. Choi, B. H. Hong, *Nature* **2009**, *457*, 706.
[6] S. Bae, H. Kim, Y. Lee, X. Xu, J.-S. Park, Y. Zheng, J. Balakrishnan, T. Lei, H. R. Kim, Y. I. Song, Y.-J. Kim, K. S. Kim, B. Ozyilmaz, J.-H. Ahn, B. H. Hong, S. Iijima, *Nat. Nanotechnol.* **2010**, *5*, 574.
[7] F. Bonaccorso, Z. Sun, T. Hasan, A. C. Ferrari, *Nat. Photonics* **2010**, *4*, 611.
[8] Y.-P. Sun, B. Zhou, Y. Lin, W. Wang, K. A. S. Fernando, P. Pathak, M. J. Meziani, B. A. Harruff, X. Wang, H. Wang, P. G. Luo, H. Yang, M. E. Kose, B. Chen, L. M. Veca, S.-Y. Xie, *J. Am. Chem. Soc.* **2006**, *128*, 7756.
[9] J. Shen, Y. Zhu, C. Chen, X. Yang, C. Li, *Chem. Commun.* **2011**, *47*, 2580.
[10] D. Pan, J. Zhang, Z. Li, M. Wu, *Adv. Mater.* **2010**, *22*, 734.
[11] S.-T. Yang, X. Wang, H. Wang, F. Lu, P. G. Luo, L. Cao, M. J. Meziani, J.-H. Liu, Y. Liu, M. Chen, Y. Huang, Y.-P. Sun, *J. Phys. Chem. C* **2009**, *113*, 18110.
[12] L. Cao, X. Wang, M. J. Meziani, F. Lu, H. Wang, P. G. Luo, Y. Lin, B. A. Harruff, L. M. Veca, D. Murray, S.-Y. Xie, Y.-P. Sun, *J. Am. Chem. Soc.* **2007**, *129*, 11318.
[13] A. Ananthanarayanan, X. Wang, P. Routh, B. Sana, S. Lim, D.-H. Kim, K.-H. Lim, J. Li, P. Chen, *Adv. Funct. Mater.* **2014**, *24*, 3021.
[14] P. Gao, K. Ding, Y. Wang, K. Ruan, S. Diao, Q. Zhang, B. Sun, J. Jie, *J. Phys. Chem. C* **2014**, *118*, 5164.
[15] X. Yan, X. Cui, B. Li, L.-S. Li, *Nano Lett.* **2010**, *10*, 1869.
[16] V. Gupta, N. Chaudhary, R. Srivastava, G. D. Sharma, R. Bhardwaj, S. Chand, *J. Am. Chem. Soc.* **2011**, *133*, 9960.
[17] P. Mirtchev, E. J. Henderson, N. Soheilnia, C. M. Yip, G. A. Ozin, *J. Mater. Chem.* **2012**, *22*, 1265.
[18] W. Kwon, G. Lee, S. Do, T. Joo, S.-W. Rhee, *Small* **2014**, *10*, 506.
[19] X. Li, Y. Liu, X. Song, H. Wang, H. Gu, H. Zeng, *Angew. Chem. Int. Ed.* **2015**, *54*, 1759.
[20] M. Sun, S. Qu, Z. Hao, W. Ji, P. Jing, H. Zhang, L. Zhang, J. Zhao, D. Shen, *Nanoscale* **2014**, *6*, 13076.

[21] W. Kwon, Y.-H. Kim, C.-L. Lee, M. Lee, H. C. Choi, T.-W. Lee, S.-W. Rhee, *Nano Lett.* **2014**, *14*, 1306.
[22] F. Wang, Y.-h. Chen, C.-y. Liu, D.-g. Ma, *Chem. Commun.* **2011**, *47*, 3502.
[23] C. Xie, B. Nie, L. Zeng, F.-X. Liang, M.-Z. Wang, L. Luo, M. Feng, Y. Yu, C.-Y. Wu, Y. Wu, S.-H. Yu, *ACS Nano* **2014**, *8*, 4015.
[24] Q. Zhang, J. Jie, S. Diao, Z. Shao, Q. Zhang, L. Wang, W. Deng, W. Hu, H. Xia, X. Yuan, S.-T. Lee, *ACS Nano* **2015**, *9*, 1561.
[25] J. Liu, Y. Liu, N. Liu, Y. Han, X. Zhang, H. Huang, Y. Lifshitz, S.-T. Lee, J. Zhong, Z. Kang, *Science* **2015**, *347*, 970.
[26] D. Chao, C. Zhu, X. Xia, J. Liu, X. Zhang, J. Wang, P. Liang, J. Lin, H. Zhang, Z. X. Shen, H. J. Fan, *Nano Lett.* **2015**, *15*, 565.
[27] Y. Zhu, X. Ji, C. Pan, Q. Sun, W. Song, L. Fang, Q. Chen, C. E. Banks, *Energ. Environ. Sci.* **2013**, *6*, 3665.
[28] L. Wang, Y. Wang, T. Xu, H. Liao, C. Yao, Y. Liu, Z. Li, Z. Chen, D. Pan, L. Sun, M. Wu, *Nat. Commun.* **2014**, *5*, 5357.
[29] X. Li, S. Zhang, S. A. Kulinich, Y. Liu, H. Zeng, *Sci. Rep.* **2014**, *4*, 4976.
[30] X. T. Zheng, A. Ananthanarayanan, K. Q. Luo, P. Chen, *Small* **2014**, *14*, 1620.
[31] Z. Zhang, J. Zhang, N. Chen, L. Qu, *Energ. Environ. Sci.* **2012**, *5*, 8869.
[32] J. Shen, Y. Zhu, X. Yang, C. Li, *Chem. Commun.* **2012**, *48*, 3686.
[33] S. Qu, X. Wang, Q. Lu, X. Liu, L. Wang, *Angew. Chem. Int. Ed.* **2012**, *51*, 12215.
[34] H. Li, X. He, Z. Kang, H. Huang, Y. Liu, J. Liu, S. Lian, C. H. A. Tsang, X. Yang, S.-T. Lee, *Angew. Chem. Int. Ed.* **2010**, *49*, 4430.
[35] Y. Dai, H. Long, X. Wang, Y. Wang, Q. Gu, W. Jiang, Y. Wang, C. Li, T. H. Zeng, Y. Sun, J. Zeng, *Part. Part. Syst. Char.* **2014**, *31*, 597.
[36] R. Liu, D. Wu, X. Feng, K. Müllen, *J. Am. Chem. Soc.* **2011**, *133*, 15221.
[37] X. Zhou, Y. Zhang, C. Wang, X. Wu, Y. Yang, B. Zheng, H. Wu, S. Guo, J. Zhang, *ACS Nano* **2012**, *6*, 6592.
[38] Y. Li, Y. Zhao, H. Cheng, Y. Hu, G. Shi, L. Dai, L. Qu, *J. Am. Chem. Soc.* **2012**, *134*, 15.
[39] S. Zhu, J. Zhang, S. Tang, C. Qiao, L. Wang, H. Wang, X. Liu, B. Li, Y. Li, W. Yu, X. Wang, H. Sun, B. Yang, *Adv. Funct. Mater.* **2012**, *22*, 4732.
[40] S. Zhu, S. Tang, J. Zhang, B. Yang, *Chem. Commun.* **2012**, *48*, 4527.
[41] L. Wang, S.-J. Zhu, H.-Y. Wang, S.-N. Qu, Y.-L. Zhang, J.-H. Zhang, Q.-D. Chen, H.-L. Xu, W. Han, B. Yang, H.-B. Sun, *ACS Nano* **2014**, *8*, 2541.
[42] L. Bao, Z.-L. Zhang, Z.-Q. Tian, L. Zhang, C. Liu, Y. Lin, B. Qi, D.-W. Pang, *Adv. Mater.* **2011**, *23*, 5801.
[43] D. Qu, M. Zheng, P. Du, Y. Zhou, L. Zhang, D. Li, H. Tan, Z. Zhao, Z. Xie, Z. Sun, *Nanoscale* **2013**, *5*, 12272.
[44] W. Wei, C. Xu, L. Wu, J. Wang, J. Ren, X. Qu, *Sci. Rep.* **2014**, *4*, 3564.
[45] Y. Dong, H. Pang, H. B. Yang, C. Guo, J. Shao, Y. Chi, C. M. Li, T. Yu, *Angew. Chem. Int. Ed.* **2013**, *125*, 7954.
[46] H. Li, X. He, Y. Liu, H. Huang, S. Lian, S.-T. Lee, Z. Kang, *Carbon* **2011**, *49*, 605.
[47] L. Tang, R. Ji, X. Cao, J. Lin, H. Jiang, X. Li, K. S. Teng, C. M. Luk, S. Zeng, J. Hao, S. P. Lau, *ACS Nano* **2012**, *6*, 5102.
[48] S. K. Bhunia, A. Saha, A. R. Maity, S. C. Ray, N. R. Jana, *Sci. Rep.* **2013**, *3*, 1473.
[49] X. Tan, Y. Li, X. Li, S. Zhou, L. Fan, S. Yang, *Chem. Commun.* **2015**, *51*, 2544.
[50] Y. Liu, C.-y. Liu, Z.-y. Zhang, *J. Mater. Chem. C* **2013**, *1*, 4902.
[51] D. Pan, J. Zhang, Z. Li, C. Wu, X. Yan, M. Wu, *Chem. Commun.* **2010**, *46*, 3681.
[52] M. X. Gao, C. F. Liu, Z. L. Wu, Q. L. Zeng, X. X. Yang, W. B. Wu, Y. F. Li, C. Z. Huang, *Chem. Commun.* **2013**, *49*, 8015.
[53] S. H. Jin, D. H. Kim, G. H. Jun, S. H. Hong, S. Jeon, *ACS Nano* **2013**, *7*, 1239.
[54] J. Shang, L. Ma, J. Li, W. Ai, T. Yu, G. G. Gurzadyan, *Sci. Rep.* **2012**, 2.
[55] S. Hu, A. Trinchi, P. Atkin, I. Cole, *Angew. Chem. Int. Ed.* **2015**, *54*, 2970.
[56] Q.-L. Zhao, Z.-L. Zhang, B.-H. Huang, J. Peng, M. Zhang, D.-W. Pang, *Chem. Commun.* **2008**, *41*, 5116.
[57] S. Zhu, J. Zhang, C. Qiao, S. Tang, Y. Li, W. Yuan, B. Li, L. Tian, F. Liu, R. Hu, H. Gao, H. Wei, H. Zhang, H. Sun, B. Yang, *Chem. Commun.* **2011**, *47*, 6858.
[58] X. Wen, P. Yu, Y.-R. Toh, X. Hao, J. Tang, *Adv. Opt. Mater.* **2013**, *1*, 173.
[59] L. Wang, S.-J. Zhu, H.-Y. Wang, Y.-F. Wang, Y.-W. Hao, J.-H. Zhang, Q.-D. Chen, Y.-L. Zhang, W. Han, B. Yang, H.-B. Sun, *Adv. Opt. Mater.* **2013**, *1*, 264.
[60] F. Liu, M.-H. Jang, H. D. Ha, J.-H. Kim, Y.-H. Cho, T. S. Seo, *Adv. Mater.* **2013**, *25*, 3657.
[61] G. Eda, Y.-Y. Lin, C. Mattevi, H. Yamaguchi, H.-A. Chen, I. S. Chen, C.-W. Chen, M. Chhowalla, *Adv. Mater.* **2010**, *22*, 505.
[62] M. A. Sk, A. Ananthanarayanan, L. Huang, K. H. Lim, P. Chen, *J. Mater. Chem. C* **2014**, *2*, 6954.
[63] R. Sekiya, Y. Uemura, H. Murakami, T. Haino, *Angew. Chem. Int. Ed.* **2014**, *53*, 5619.
[64] X. Li, H. Wang, Y. Shimizu, A. Pyatenko, K. Kawaguchi, N. Koshizaki, *Chem. Commun.* **2011**, *47*, 932.
[65] Q.-L. Chen, C.-F. Wang, S. Chen, *J. Mater. Sci.* **2013**, *48*, 2352.
[66] X. Guo, C.-F. Wang, Z.-Y. Yu, L. Chen, S. Chen, *Chem. Commun.* **2012**, *48*, 2692.
[67] L.-H. Mao, W.-Q. Tang, Z.-Y. Deng, S.-S. Liu, C.-F. Wang, S. Chen, *Ind. Eng. Chem. Res.* **2014**, *53*, 6417.
[68] X. Zheng, H. Wang, Q. Gong, L. Zhang, G. Cui, Q. Li, L. Chen, F. Wu, S. Wang, *Mater. Lett.* **2015**, *143*, 290.
[69] S. Xie, S. Bao, J. Ouyang, X. Zhou, Q. Kuang, Z. Xie, L. Zheng, *Chem. Eur. J.* **2014**, *20*, 5244.
[70] W. Kwon, S. Do, J. Lee, S. Hwang, J. K. Kim, S.-W. Rhee, *Chem. Mater.* **2013**, *25*, 1893.
[71] S. Do, W. Kwon, S.-W. Rhee, *J. Mater. Chem. C* **2014**, *2*, 4221.
[72] Q. Sun, Y. A. Wang, L. S. Li, D. Wang, T. Zhu, J. Xu, C. Yang, Y. Li, *Nat. Photonics* **2007**, *1*, 717.
[73] X. Dai, Z. Zhang, Y. Jin, Y. Niu, H. Cao, X. Liang, L. Chen, J. Wang, X. Peng, *Nature* **2014**, *515*, 96.
[74] J. Liang, L. Li, X. Niu, Z. Yu, Q. Pei, *Nat. Photonics* **2013**, *7*, 817.
[75] X. Zhang, Y. Zhang, Y. Wang, S. Kalytchuk, S. V. Kershaw, Y. Wang, P. Wang, T. Zhang, Y. Zhao, H. Zhang, T. Cui, Y. Wang, J. Zhao, W. W. Yu, A. L. Rogach, *ACS Nano* **2013**, *7*, 11234.
[76] S. H. Song, M.-H. Jang, J. Chung, S. H. Jin, B. H. Kim, S.-H. Hur, S. Yoo, Y.-H. Cho, S. Jeon, *Adv. Opt. Mater.* **2014**, *2*, 1016.
[77] L. Tang, R. Ji, X. Li, G. Bai, C. P. Liu, J. Hao, J. Lin, H. Jiang, K. S. Teng, Z. Yang, S. P. Lau, *ACS Nano* **2014**, *8*, 6312.
[78] C. O. Kim, S. W. Hwang, S. Kim, D. H. Shin, S. S. Kang, J. M. Kim, C. W. Jang, J. H. Kim, K. W. Lee, S.-H. Choi, E. Hwang, *Sci. Rep.* **2014**, 4.
[79] M. Li, W. Ni, B. Kan, X. Wan, L. Zhang, Q. Zhang, G. Long, Y. Zuo, Y. Chen, *Phys. Chem. Chem. Phys.* **2013**, *15*, 18973.
[80] C. Liu, K. Chang, W. Guo, H. Li, L. Shen, W. Chen, D. Yan, *Appl. Phys. Lett.* **2014**, *105*, 073306.
[81] Y.-Q. Zhang, D.-K. Ma, Y.-G. Zhang, W. Chen, S.-M. Huang, *Nano Energy* **2013**, *2*, 545.
[82] M. Dutta, S. Sarkar, T. Ghosh, D. Basak, *The J. Phys. Chem. C* **2012**, *116*, 20127.

[83] Y. Qin, Y. Cheng, L. Jiang, X. Jin, M. Li, X. Luo, G. Liao, T. Wei, Q. Li, *ACS Sustainable Chem. Eng.* **2015**.
[84] X. Shen, B. Sun, D. Liu, S.-T. Lee, *J. Am. Chem. Soc.* **2011**, *133*, 19408.
[85] J. Briscoe, A. Marinovic, M. Sevilla, S. Dunn, M. Titirici, *Angew. Chem. Int. Ed.* **2015**, *54*, 4463.
[86] R. Narayanan, M. Deepa, A. K. Srivastava, *J. Mater. Chem. A* **2013**, *1*, 3907.
[87] I. Mihalache, A. Radoi, M. Mihaila, C. Munteanu, A. Marin, M. Danila, M. Kusko, C. Kusko, *Electrochim. Acta* **2015**, *153*, 306.
[88] X. Fang, M. Li, K. Guo, J. Li, M. Pan, L. Bai, M. Luoshan, X. Zhao, *Electrochim. Acta* **2014**, *137*, 634.
[89] H. Ming, Z. Ma, Y. Liu, K. Pan, H. Yu, F. Wang, Z. Kang, *Dalton* **2012**, *41*, 9526.
[90] H. Yu, Y. Zhao, C. Zhou, L. Shang, Y. Peng, Y. Cao, L.-Z. Wu, C.-H. Tung, T. Zhang, *J. Mater. Chem. A* **2014**, *2*, 3344.
[91] T.-F. Yeh, C.-Y. Teng, S.-J. Chen, H. Teng, *Adv. Mater.* **2014**, *26*, 3297.
[92] X. Yu, R. Liu, G. Zhang, H. Cao, *Nanotechnology* **2013**, *24*, 335401.
[93] H. Li, X. Zhang, D. R. MacFarlane, *Adv. Energy Mater.* **2015**, *5*, 1077.
[94] R. Liu, H. Huang, H. Li, Y. Liu, J. Zhong, Y. Li, S. Zhang, Z. Kang, *ACS Catal.* **2014**, *4*, 328.
[95] W. Wu, L. Zhan, W. Fan, J. Song, X. Li, Z. Li, R. Wang, J. Zhang, J. Zheng, M. Wu, H. Zeng, *Angew. Chem. Int. Ed.* **2015**, *54*, 6540.
[96] N. J. Jeon, J. H. Noh, W. S. Yang, Y. C. Kim, S. Ryu, J. Seo, S. I. Seok, *Nature* **2015**, *517*, 476.
[97] X. Li, Y. Li, H. Zeng, *Sci. Adv. Mater.* **2013**, *5*, 1585.
[98] A. W. Blakers, A. Wang, A. M. Milne, J. Zhao, M. A. Green, *Appl. Phys. Lett.* **1989**, *55*, 1363.
[99] L. Shen, Q. Che, H. Li, X. Zhang, *Adv. Funct. Mater.* **2014**, *24*, 2630.
[100] S. Peng, L. Li, C. Li, H. Tan, R. Cai, H. Yu, S. Mhaisalkar, M. Srinivasan, S. Ramakrishna, Q. Yan, *Chem. Commun.* **2013**, *49*, 10178.
[101] H. Xia, C. Hong, B. Li, B. Zhao, Z. Lin, M. Zheng, S. V. Savilov, S. M. Aldoshin, *Adv. Funct. Mater.* **2015**, *25*, 627.
[102] H. Chen, J. Jiang, L. Zhang, D. Xia, Y. Zhao, D. Guo, T. Qi, H. Wan, *J. Power Sources* **2014**, *254*, 249.
[103] Y. Liu, N. Zhang, L. Jiao, Z. Tao, J. Chen, *Adv. Funct. Mater.* **2015**, *25*, 214.
[104] L. Y. Lim, N. Liu, Y. Cui, M. F. Toney, *Chem. Mater.* **2014**, *26*, 3739.
[105] Y. Hu, Y. Zhao, G. Lu, N. Chen, Z. Zhang, H. Li, H. Shao, L. Qu, *Nanotechnology* **2013**, *24*, 195401.
[106] W. Liu, X. Yan, J. Chen, Y. Feng, Q. Xue, *Nanoscale* **2013**, *5*, 6053.
[107] J. Huang, B. G. Sumpter, V. Meunier, *Angew. Chem. Int. Ed.* **2008**, *47*, 520.
[108] Q. Chen, Y. Hu, C. Hu, H. Cheng, Z. Zhang, H. Shao, L. Qu, *Phys. Chem. Chem. Phys.* **2014**, *16*, 19307.
[109] L. Lv, Y. Fan, Q. Chen, Y. Zhao, Y. Hu, Z. Zhang, N. Chen, L. Qu, *Nanotechnology* **2014**, *25*, 235401.
[110] W.-W. Liu, Y.-Q. Feng, X.-B. Yan, J.-T. Chen, Q.-J. Xue, *Adv. Funct. Mater.* **2013**, *23*, 4111.
[111] C. Zhu, D. Chao, J. Sun, I. M. Bacho, Z. Fan, C. F. Ng, X. Xia, H. Huang, H. Zhang, Z. X. Shen, G. Ding, H. J. Fan, *Adv. Mater. Interfaces* **2015**, 2, 499.
[112] B. Kong, A. Zhu, C. Ding, X. Zhao, B. Li, Y. Tian, *Adv. Mater.* **2012**, *24*, 5844.
[113] Q. Wang, X. Huang, Y. Long, X. Wang, H. Zhang, R. Zhu, L. Liang, P. Teng, H. Zheng, *Carbon* **2013**, *59*, 192.
[114] L. Zhou, Y. Lin, Z. Huang, J. Ren, X. Qu, *Chem. Commun.* **2012**, *48*, 1147.
[115] W. F. Zhang, H. Zhu, S. F. Yu, H. Y. Yang, *Adv. Mater.* **2012**, *24*, 2263.
[116] S. Qu, X. Liu, X. Guo, M. Chu, L. Zhang, D. Shen, *Adv. Funct. Mater.* **2014**, *24*, 2689.
[117] W. Kwon, S. Do, D. C. Won, S.-W. Rhee, *ACS Appl. Mater. Interfaces* **2013**, *5*, 822.